NUMERICAL INVESTIGATION OF A HYBRID PHOTOVOLTAIC THERMAL PVT MODULE

A Thesis by

Taspia Shawkat Chowdhury
Mita Noor Hasan Mita
Fatima Tasneem Mohsin

Department of Mechanical and Production Engineering
Islamic University of Technology

May (2022)

NUMERICAL INVESTIGATION OF A HYBRID PHOTOVOLTAIC THERMAL PVT MODULE

Taspia Shawkat Chowdhury (170011025)
Mita Noor Hasan Mita (170011062)
Fatima Tasneem Mohsin (170011072)

Submitted in Partial Fulfillment
of the Requirements
for the Degree of
Bachelor of Science in Mechanical Engineering

DEPARTMENT OF MECHANICAL AND PRODUCTION ENGINEERING

May (2022)

CERTIFICATE OF RESEARCH

This thesis titled "NUMERICAL INVESTIGATION OF A HYBRID PHOTOVOLTAIC THERMAL PVT MODULE" submitted by TASPIA SHAWKAT CHOWDHURY (170011025), MITA NOOR HASAN MITA (170011062) and FATIMA TASNEEM MOHSIN (170011072) has been accepted as satisfactory in partial fulfillment of the requirement for the Degree of Bachelor of Science in Mechanical Engineering.
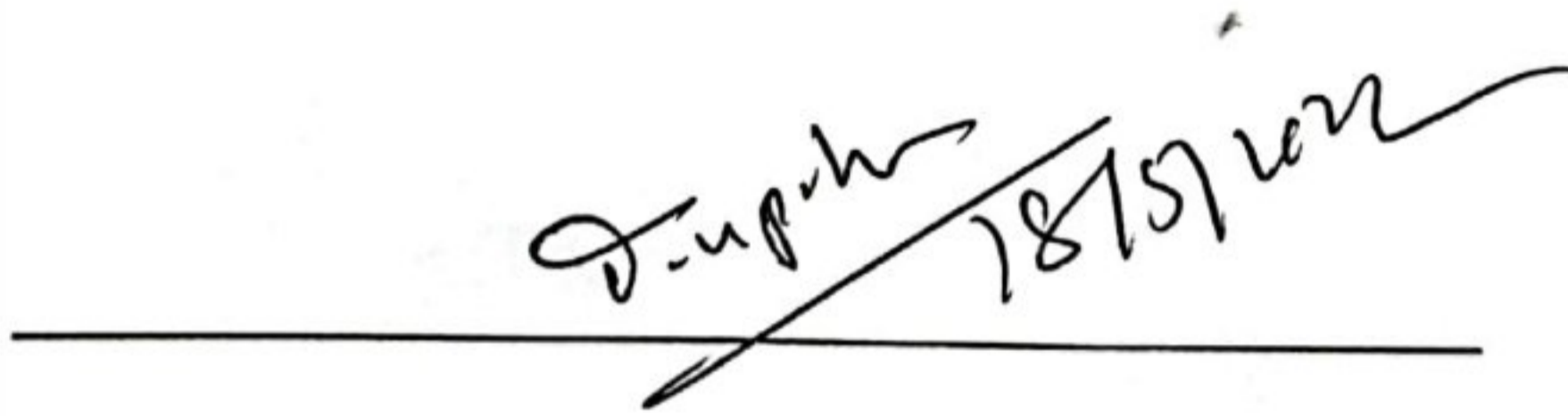
Supervisor

Dr. Arafat Ahmed Bhuiyan

Associate Professor

Department of Mechanical and Production Engineering
(MPE)

Head of the Department

Prof. Dr. Md. Anayet Ullah Patwari

Professor

Department of Mechanical and Production Engineering
(MPE)

Islamic University of Technology (IUT)

DECLARATION

I hereby declare that this thesis entitled "NUMERICAL INVESTIGATION OF A HYBRID PHOTOVOLTAIC THERMAL PVT MODULE" is an authentic report of our study carried out as requirement for the award of degree B.Sc. (Mechanical Engineering) at Islamic University of Technology, Gazipur, Dhaka, under the supervision of Dr. Arafat Ahmed Bhuiyan, Associate Professor, MPE, IUT in the year 2022

The matter embodied in this thesis has not been submitted in part or full to any other institute for award of any degree.

Taspia

Taspia Shawkat Chowdhury

170011025

Mita Noor

Mita Noor Hasan Mita

170011062

Fatima Tasneem Mohsin

170011072

Acknowledgments

ABSTRACT

Over 173,000 terawatts of solar radiation continuously strike the Earth's atmosphere however, most of this energy is reflected or absorbed and is lost due to insufficient space and technology required to harness the solar energy and generate electricity. Photovoltaic (PV) solar panels are widely used globally to receive light energy from solar irradiance and convert it to electricity. PV cells are designed to absorb as much as 80 percent of the insolation energy however, due to structural limitations only 10-15 % of this incident solar radiation is converted to electricity with most of this absorbed energy converting to heat and raising the temperature of the entire module and greatly reducing the efficiency of electricity generation. This undesirable reduction in electrical efficiency is avoided by the addition of a heat recovery system to the PV module to cool the panel and effectively extract waste heat to enhance both thermal and electrical efficiency. Such modified PV modules are known as hybrid PV module or Photovoltaic thermal systems. The primary purpose of this research is to numerically validate the effectiveness of various ribbed surfaces in enhancing the thermal efficiency of the dual hybrid PVT system by simultaneously using both air and liquid water as cooling fluids. In addition, the effect of water and air velocities on thermal efficiency have also been observed by monitoring the temperatures at water outlet. The findings indicate significant reduction in the water outlet temperature with increasing water velocity and decreasing air velocity drawing the conclusion that the air velocity maximized, and water should be passed at a low velocity to achieve higher heat transfer rates. The utilization of ribbed surfaces substantially improved thermal performance with the semicircular and triangular ribbed surfaces achieving higher water outlet temperature at all solar heat flux throughout the day. Highest water outlet temperature and thus heat transfer was observed to be occurred at 1:00 P.M when the heat flux from the sun is maximum. The numerical findings successfully conformed with the data obtained from the experiment and conform to the results from previous research works. Finally, this study provides a comprehensive comparison between the different geometries of the PVT module and determines the optimum operating conditions for optimized thermal efficiency of the PVT module.

Keywords: PVT module, thermal performance, numerical analysis, electrical efficiency, ribbed surfaces, solar energy, ANSYS Fluent, coolant.

Table of Contents

LIST OF FIGURES

LIST OF TABLES

NOMENCLATURE

PVT	Photo Voltaic Thermal
v_w	Kinematic viscosity of water
ρ_w	Density of water
C_p	Mass specific heat capacity at constant pressure (J kg^{-1} K^{-1})
p	Pressure (Pa)
$\dot{q}$	Heat flux vector per unit area (W m^{-2})
$\dot{q}_v$	Heat sources per unit volume (W m^{-3})
S	Strain rate tensor (s^{-1})
T	Absolute temperature (K)
t	Time (s)
u	Velocity vector (m s^{-1})
V	Volume (m^3)
ρ	Density (kg m^{-3})
τ	Viscous stress tensor (Pa)
∇	Nabla vector (operator)
$\dot{m}$	Mass flow rate of fluid (kg/s)
G	Solar radiation intensity (W/m^2)
A_a	Area of the aperture (m^2)
Q_a	Heat energy absorbed
η_{th}	Thermal Efficiency
η_{pv}	Electrical Efficiency
k	Thermal Conductivity (W/m.K)

Chapter 01: INTRODUCTION

1.1 Background and Overview

In the past few decades due to the immense industrialization and massive use of modern technology, there has been a sudden rise in the global power demand with developing countries energy usage exceeding that of developed countries. This rapid increase in energy requirements has led to critical environmental issues and affecting the economic conditions of countries. Pollution has exceeded safety standards and global warming, ozone layer destruction, carbon monoxide pollution has become the eminent result. Furthermore, natural resource depletion, over exploitation of fuels, deforestation and rising price of non-renewable resources has led to countries becoming increasingly aware of their power consumption and switching to utilizing renewable based resources. In addition to cope up with the rising global power demand, the utilization of renewable based resources such as solar energy, wind energy, hydro energy, etc. has become essential.

In the last decade the utilization of renewable based resources has increased by up to 42% and solar energy is the third largest renewable resource contributor to the global power demand. In 2020, as much as 3.3 percent of the world's electricity generation was from solar energy alone and its usage is rapidly growing. Solar energy is one of the most abundant forms of renewable energy and is presently gaining more popularity both as a sustainable and well as renewable energy source. Sunlight is one of the cleanest energy resources resulting in zero pollution in its production as well as one of the most ample and free sources of energy available globally. Due to its sustainability as well as immense availability, utilization of solar energy to generate electricity and power is becoming increasing widespread.

1.2 Brief introduction of Photovoltaic Module

Photovoltaic panels or PV modules are one of the most commonly used means of harnessing solar radiation to generate electricity. PV cells are composed of an array of monocrystalline or polycrystalline silicon crystal wafers. This silicon wafers are the primary component of a PV cell. A typical solar panel is composed of several layers with interconnected PV cells connected by copper strips. These interconnected PV cells

are covered by an encapsulation foil or EVA sheet layer on both sides to protect them from sudden shocks, vibrations, moisture and dirt. These EVA sheets are covered by a tempered glass and finally an aluminum frame to provide support.
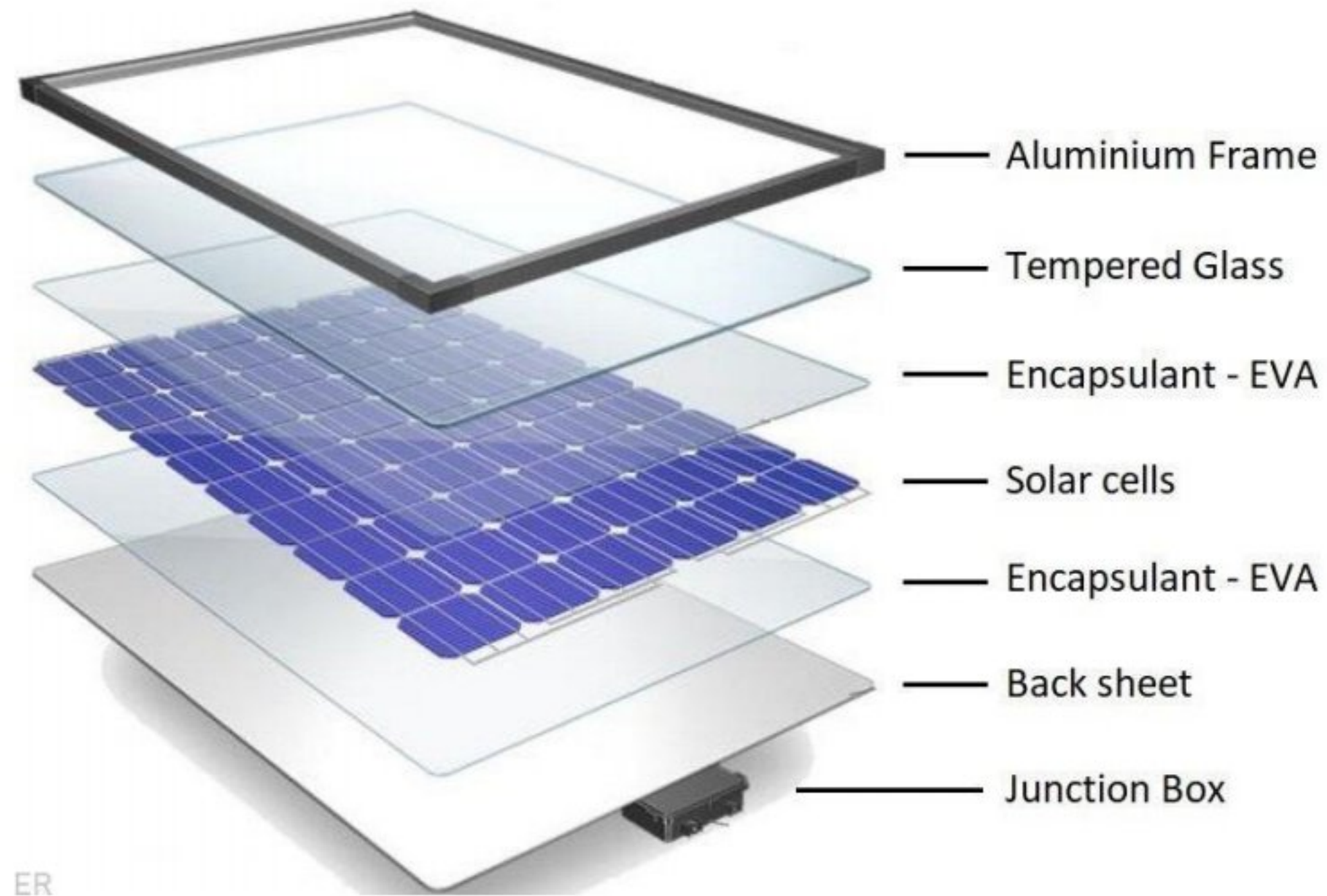
Figure 1: Major components of a Photovoltaic panel.[1]
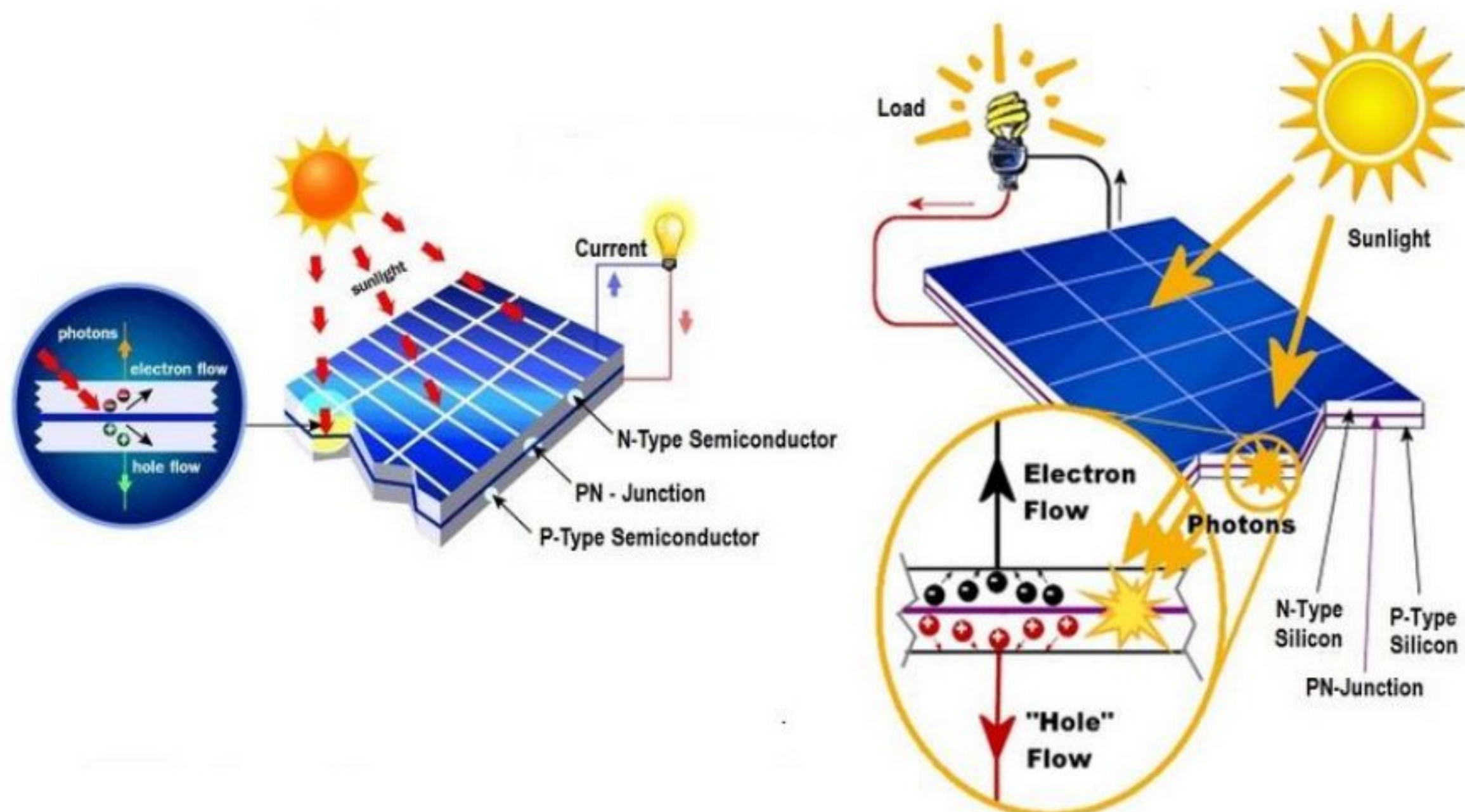
Figure 2: Operational Principle of a Solar PV panel.[2]

A typical PV cell consists of two layers of silicon crystal, the top layer doped with phosphorous atoms to create free valence electrons (n type doping), and a bottom layer doped with boron atom resulting in hole formation (p type doping) resulting in a P-N junction. When these two regions are joined together, some electrons from the N side transfer to the P region combing with the holes and creating the depletion region. Due to electron transfer, N region seems to be positively charged while the P region is negatively charged with an electric force between them resulting in a driving force. When sunlight hits the PV cell, photons having sufficient energy creates pairs of electron and hole in the depletion region which are attracted towards opposite junctions due to the driving force and creates a sufficiently high potential difference between the two regions. If a load is connected between the two regions electricity is generated due to flow of electrons.

1.3 Problem Statement

However, one of the major problems of PV modules are its low efficiency particularly at high temperatures. In PV Modules only 6-15 % of the incident solar radiation is converted into electrical energy and the greater percentage gets reflected or converted into heat and deteriorates the electrical efficiency.[3] Recent advancements in Photovoltaic (PV) systems can convert more that 18% of the absorbed insolation energy into electricity, however the rest of the insolation energy is converted to heat and significantly raises the temperature of the PV cells. Recent research shows that the efficiency of the solar PV system is severely affected when the temperature of the panel rises more than standard requirements of 25°C with the electrical efficiency of the cell falling by 0.3- 0.65 % for every 1°C rise in PV module temperature.[4][5]. This is because semiconductors such as silicon provides greater resistance to current flow at higher temperatures leading to lower electrical power production.

Therefore, it is essential to implement a method to reduce this increasing PV module temperature and control it within optimal conditions to maximize electrical efficiency. Tremendous research and studies have been conducted to manage this rising solar panel temperatures and there has been remarkable progress in the recent years. One of the commonly used means of achieving this is by extracting the surface heat from PV panels using a coolant. The most widely implemented coolants are air and water which are used for extracting the thermal energy from the PV modules and utilize it for heat

requirements of domestic and industrial processes as well as drying application.

These modified PV panels used to control the temperature of PV cells within optimal range are known as Photovoltaic thermal collectors, PVT modules or Hybrid PV modules.

1.4 Working Principle of a PVT Module

PVT system or hybrid solar panels are a technology used to simultaneously generate usable thermal energy and electricity from light energy.[6]–[9] They can be defined to be a combination of both a photovoltaic system and a thermal collector supplying continuous cool working fluid. Such systems save space eliminating the need of two separate systems and provide greater performances in terms of combined efficiency and multiple energy outputs.[10][11]

The main construction of a PVT system is dependent on a variety of factors such as the type of coolant, shape and size of the collector, presence of ribs and fins, electrical and thermal efficiency requirements, PV cell material, absorber plate type and operating conditions such a temperature, and fluid flow type.

Solar PVT systems can be broadly classified according to the cooling fluids used:
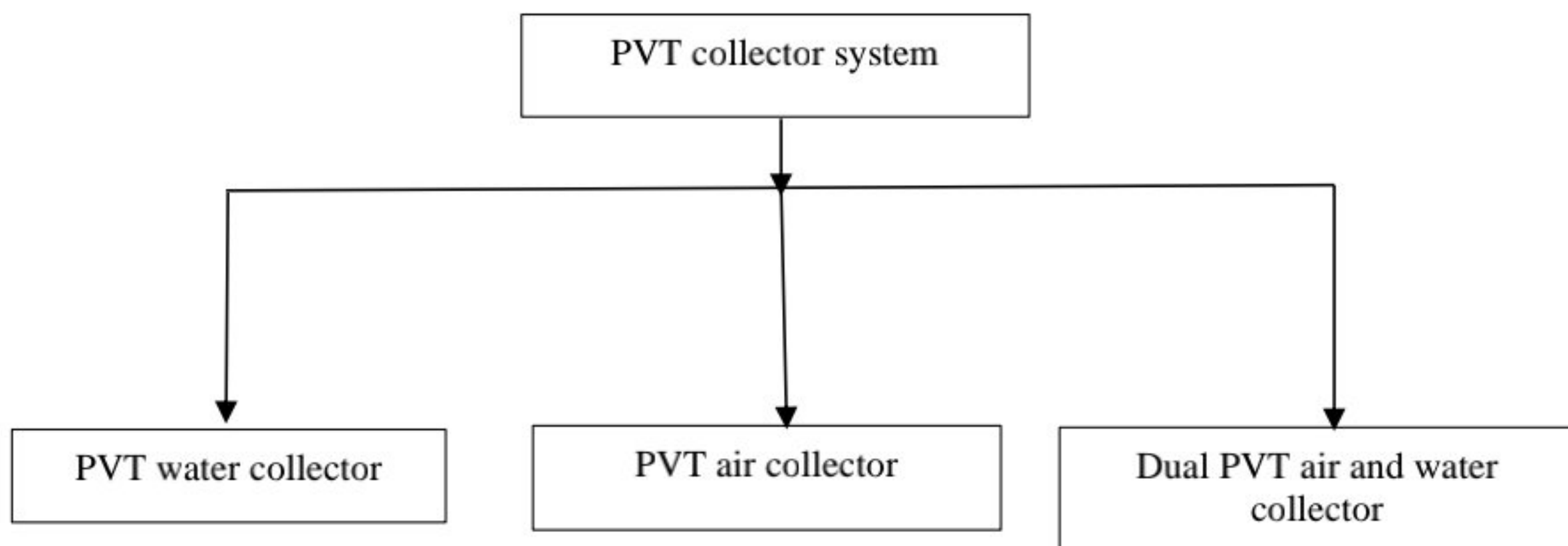
Figure 3: Classification of PVT Collector System

The main objective of PVT collectors are to effectively enhance electrical performances of PV cells and simultenously produce hot air or water for furthur usage. Recent studies have shown water or liquid based coolants to be better at heat extraction than air particulary due to its high heat capacity.[12]

4
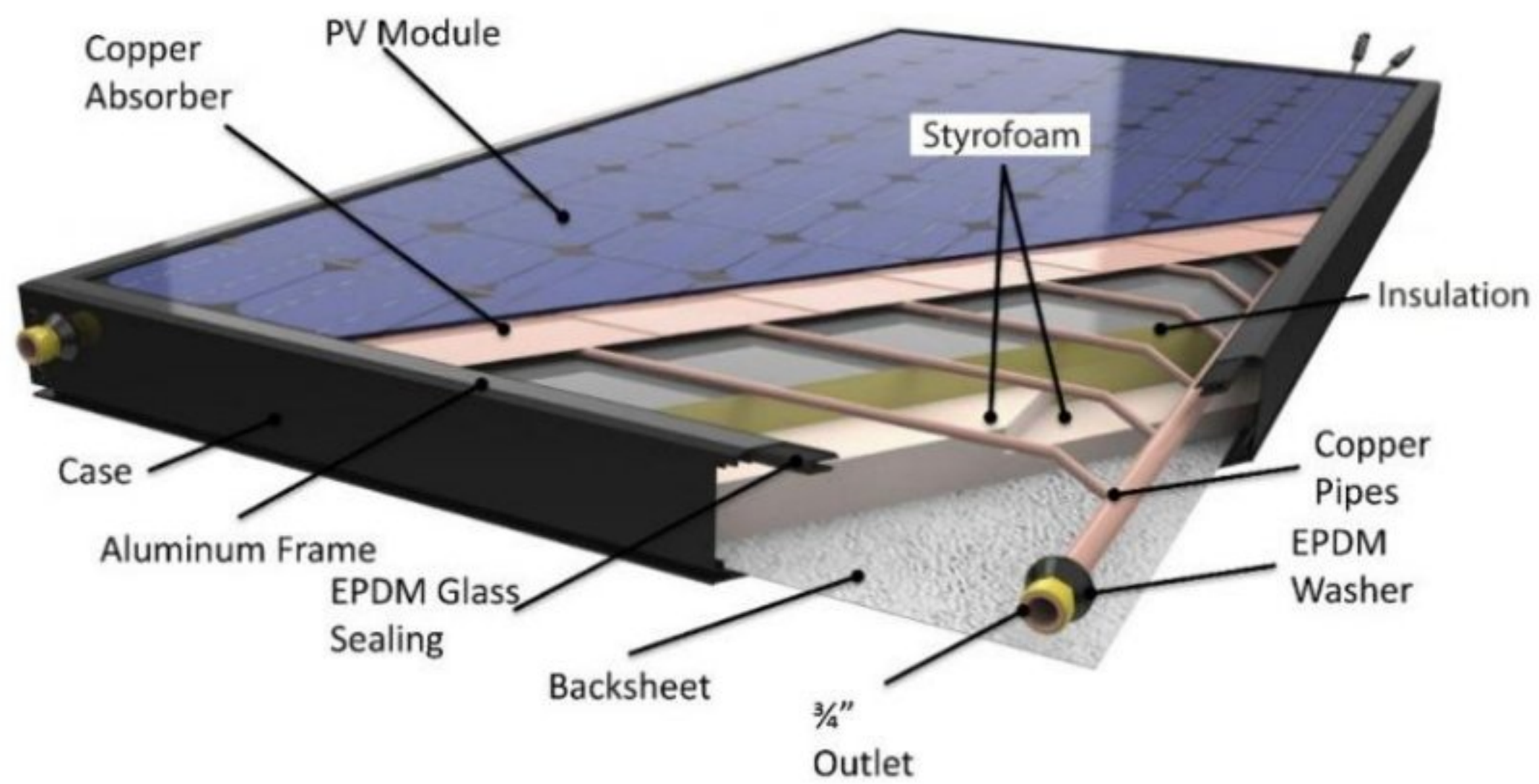
Figure 4: Typical Photovoltaic thermal collector.[13]

This study simulates a dual hybrid PVT system with and without ribbed surfaces. In this numerical investigation both air and water are used to effectively reduce PV cell surface temperature and in addition provide hot water for domestic use and hot air for drying and space heating. When solar radiation is absorbed by the PV panel, its temperature significantly rises. Cold water is supplied in cooper pipes embedded to the absorber plate and passed through the bottom surface of the PV panel to absorb the thermal heat and reduce its temperature. Moreover, a simultaneous and continuous supply of cool atmospheric air is maintained to successfully absorb the heat from the absorber plates as well as achieve hot air. The utilization of both air and water as cooling fluids will significantly raise thermal efficiency and improve the electrical performance of the whole system.

1.5 Objectives and Scopes

The major objective of this work is to numerically validate the experimental results of the reference paper and in addition analyze the effectiveness of the various geometries as well as the impact of water velocity and air velocity in achieving greater thermal and electrical efficiency. Moreover, this purpose of this research is to numerically analyze the effects of different shapes of ribbed surfaces on the thermal performance of PVT modules in terms of thermal efficiency as well as determine the effectiveness of ribbed surfaces in enhancing heat transfer to the cooling fluids. The thermal performance of different ribbed surfaces has been thoroughly studied and examined through ANSYS simulations. The variations of thermal efficiency with respect to the change in water and air velocities have been observed numerically and graphically and the results of simulations have been validated with previous research works and verified based on the findings of theoretical concepts. Furthermore, the variation of the change in temperature of the water coolant throughout the day has been examined and validated against the experimental data of the reference paper as well as past research papers. Finally, the primary scope of this study was to find the optimum configuration and operating conditions for optimized thermal efficiency of the hybrid PVT module.

Chapter 02: LITERATURE REVIEW

2.1 Review on previous Experimental Research

Jin et al. [14] performed an experiment to analyze the effect of rectangular air collector on the thermal and electrical efficiency of PVT module and found that incorporating air collector enhanced both electrical and thermal efficiencies with overall efficiency up to 64.72%. He also observed the influence of the mass flow rate of air on thermal efficiency and found the thermal efficiency to improve by changing the mass flow rate of air until a certain optimum value and is higher when air tunnel is incorporated.

Alfegi et al. [15] experimentally investigated a single pass PVT with double ducted air collector incorporated with compound parabolic collector (CPC) with added fins. He analyzed how the electrical and thermal efficiency at a fixed solar heat flux of 400 W/m^2 is affected by air mass flow rate. The results suggested that higher mass flow rate of air enhances both electrical and thermal efficiency with combined efficiency increasing from 27.50 to 40.044% and incorporating CPC and fins greatly improved electric power production.

Rawat et al. [16] developed a flat plate Photovoltaic Thermal water collector system at Bhopal and evaluated its performances experimentally. He found that the electrical efficiency of the PVT collector did not change considerably for constant water mass flow rate of 0.002 kg/sec. However, both the thermal efficiency and overall efficiency of the system enhanced significantly up to 50.1% and 73% respectively.

Bilbao et al. [17] developed an improvised simple and cost-effective PVT water module and determined its sustainability for developing countries. The designed PVT collector utilized polycarbonate collector with PVC pipes as water heat exchangers and the results were compared against a standard PV module. Furthermore, the possible deterioration in electrical performance in stagnation conditions was analyzed. The results suggested a 5 % increase in electricity production of the proposed model sufficient to power the electric motor and maintain self-sustainability of the system but a significant decrease in performance (9-10%) in stagnant conditions.

Gangadevi et al. [3] experimentally showed that typical solar cells have 6-15 % electrical efficiency but after incorporating PV/T system electrical efficiency increases. First, they used water as coolant in the hybrid solar system. But the novelty of their work is using nanofluid as a coolant afterward to compare between the two different

coolants. Here nanofluid has high heat transfer characteristics. By introducing nanofluid (Al_2O_3/water) to the system both the thermal efficiency and electrical efficiency have been significantly increased.

Dupeyrat et al. [18] experimentally conducted an research to improve the thermal properties of hybrid PV-thermal collector. The global efficiency of the PV-Thermal system is more than 87% as the electrical efficiency is 8.7% and the thermal efficiency is 79%.

Touafek et al. [19] experimentally conducted an research of a hybrid PV-Thermal System and a typical PV System. They detected an enhancement of electrical efficiency because of introducing the thermal system. They further proved that thermal efficiency could be increased by incorporating glazing. But in that case electrical efficiency drops. Therefore, a trade-off between them must be attempted based on the user's demand.

Chow et al. [20] examined the appropriateness of incorporating a glazed or unglazed PV-Thermal collector. After researching they discovered that unglazed one provided better outputs such as increasing cell efficiency, mass of water to area collector ratio, packing factor etc.

Fujisawa et al. [21] designed a hybrid PV/T panel consisting of a liquid heating system where the PV cells are of mono-Si. They implemented exergy theory concepts. They calculated the annual performance of a PV module, liquid-heating solar panel, single-glazing solar collector (mono-Si based) and unglazed solar collector. After the evaluation they found that the best one based on overall energy gain in the single-glazing solar collector. Second is SWC and the third, fourth are unglazed and PV module respectively. Based on exergy analysis the best one is unglazed, and the others are PV module, single-glazed and SWC.

Tonui et al. [22] reveals that the temperature gain is higher in case of forced circulation of air than natural circulation resulting in increased thermal efficiency. Furthermore, modifications in PVT module like FIN, TMS also yield greater thermal efficiency. The temperature rise was investigated both under natural and forced circulation of the air coolant. Even though the FIN system provides greater thermal output compared to TMS system, both the modified systems provide lesser back wall temperature than the Reference system.

Ruobing et al. [23] developed a new kind of hybrid PVT collector consisting of graphite and compared that with the typical photovoltaic panel. They evaluated and compared these two systems in terms of output power, temperatures at the backplane and tank,

the inlet and outlet temperature etc. The Photovoltaic or thermal performance of the Photovoltaic thermal collector equipped with graphite was assessed based on electrical efficiency, thermal efficiency, and primary efficiency for energy saving. The results indicate that even though the backplane temperature of PVT collector with graphite was stable, the backplane temperature of the PV panel was influenced by the solar radiation. The results suggest that if the back plane temperature is reduced, the electrical efficiency of the PVT Collector consisting of graphite will be increased. The inlet temperature seems to increase as the tank temperature increases. After the inlet temperature has enhanced to the peak point, the temperature at the outlet tends to be gradually stable. It's also concluded that the lower the inlet temperature, the higher will be the thermal efficiency. The results also suggest that the average electrical efficiency for the PVT collector equipped with the graphite is greater in comparison to the conventional PV panel.

Md Rezwanul Karim et al. [24] experimented with a dual PVT module, employing TMS and painted black ribbed surfaces to increase the thermal efficiency, also observed the variations in temperature gain with varying shapes of ribs. Natural convection is employed instead of forced convection which results into increased overall system efficiency and electrical output. The average temperature gain for both the water and air was found to be better with squared ribs than with the flat plate, and highest for the triangular and semicircular ribbed surfaces. It is also observed that thermal efficiency was maximum for the triangular ribs compared to others under the same experimental conditions. However, the electrical efficiency doesn't seem to vary that much although it's found to be maximum for the triangular and semicircular ribs.

2.2 Review on previous Numerical Research

Al-Damook et al. [25] has assessed the numerical analysis of a one pass PVT air collector incorporating offset fins and compared the results to an unfinned system. The results suggest significant improvement in combined efficiency 84.7% when using offset strip fins compared to 51.2% for unfinned systems. The thermal efficiency for the system improved with increasing Reynolds number however higher flow velocities resulted in significant pressure drop.

Aste et al. [26] investigated the effect of air gaps on the performance of PVT water collector using two mathematical models. He analyzed and compared two types of PVT

water collector system, one covered that consists of two layers, a top amorphous Si layer and a bottom microcrystalline Si layer enclosed in a glass cover, and the other uncovered and validated his results using TRNSYS. The results showed almost equal combined efficiency for both modules. Thermal efficiency of the covered system was considerably greater, however, in terms of primary energy performance, the uncovered module was more effective.

Othman et al. [27] analyzed both the thermal and electrical performances of a hybrid double pass PVT air collector system incorporated with fins using mathematical models. He used two mass flow rates of air, 0.027 kg/s and 0.181 kg/s. He found that the thermal efficiency was significantly higher both theoretically and experimentally for increasing air mass flow rates. However, the rise in air temperature decreased as air mass flow rate was increased. Furthermore, fin utilization greatly enhanced both thermal and electrical efficiencies.

Hassani et al. [28] proposed a new PVT configuration utilizing two different nanofluids, an optical nanofluid that acts as a liquid optical barrier for solar radiation above the PV cells and another a thermal nanofluid to extract heat and cool the PV module. He numerically analyzed the proposed configuration for a double pass and a separate channel design for both Si as well as GaAs PV cells. The results suggested better performances with separate channels for high solar concentration systems and improved efficiencies of the PVT with the cascaded nanofluid module. Furthermore, the electrical performances of both PV cells enhanced with greater volume fraction of the coolant nanofluid.

Han et al. [29] established a mathematical model using Gambit and numerically analyzed the performance analysis of a PVT solar thermal (PVT-ST) system operating in series against a PV and ST system. He found the PV-ST system to achieve better thermal and electrical performance at reduced solar heat flux and low ambient temperatures however, the PVT-ST system performed significantly better at strong solar radiance with increased ambient temperature.

Jianyu Guo et al. [30] presented a innovative design of a hybrid PV/Thermal system, where solar cells are attached to the glass cover's bottom surface to perceive higher electrical efficiency by considering the glass cover's temperature lower compared to the temperature of absorber plate. They conducted a numerical study for comparing the characteristics of conventional and newly designed PV/T system.

Zondag et al. [31] established 4 numerical models (1D, 2D, 3D steady state models and

a 3D-dynamic model) to accurately simulate the thermal yield of a hybrid PV-Thermal system. The numerical results matched with the experimental one within 5% accuracy. For a more precise prediction of the results, time dependent model was required.

Fraisse et al. [32] researched about hybrid PV/Thermal systems incorporating water as a coolant that were implemented to merged system of direct solar-floor type. The outcomes presented that the electrical efficiency reduced about 28 percent in the glazed Photovoltaic/Thermal collectors compared to the traditional nonintegrated Photovoltaic system, but a rise of 6 percent was seen in the unglazed one. Therefore, they recommended to uncover the collector if the thermal performance was not significant in particular condition.

Bakker et al. [33] simulated the performance of a ground-coupled heat pump combined with a unglazed PV/T panel of 25 m^2 via TRNSYS. For a newly constructed one-person dwelling, this system can cover 100 % of net heat demand. For this system total investment needed are comparable to those side-by-side system consisting of 26 m^2 PV collectors and 7 m^2 solar thermal panels.

Mauricio et al. [34] compared the simultaneous operational performance of a traditional PV module with a hybrid PVT-PCM module in which phase change material is incorporated. It's observed that the daily electrical efficiency is increased resulting into an increase in total capability for extraction of solar energy in case of the PVT-PCM module. This is due to the fact that in the modular design of this type of modified solar collector consists of PCM containers in the back of the conventional PV module. A PCM container is composed of a copper coil, passing through the phase change material, which eventually leads to improved heat transfer for the working fluid. It's also found that the thermal inertia caused by the addition of PCM creates the tendency to maintain more appropriate temperatures of the PV cells, ensuring storage during the day and dissipation during the night of the thermal energy.

R.M. da Silva et al. [35] developed a thermodynamic model of a photovoltaic thermal (PVT) Solar system, via the Simulink/MATLAB platform. A sensitivity analysis is performed, which indicates that the most significant factor for improving the thermal performance is the Photovoltaic module emittance. According to the results of such analysis, some strategies have been proposed to improve the thermal performance of PVT collector.   One such strategy is that vacuum or noble gases at low pressure can be employed in order to remove the encapsulation at the inner glass, for reducing the emissivity and optical loss due to reflection. It's also revealed that this strategy leads to

a significant increase in the optical thermal efficiency, decrease in the thermal loss and enhanced temperatures of the working fluid. Since the removal of encapsulation increases the optical properties, the deterioration of electrical efficiency caused by the higher PV cell temperatures was negligibly less. Furthermore, the performance can be improved by evaluation of the vacuum PVT collector.

Chao-Yang et al. [36] established a simulation model of hybrid thermal PVT module by implementing TRANSYS tool, which is capable of predicting the system performance in different conditions of weather based on the transient and long term assessment. In this study the performance of a thermal hybrid system has a assessed in various locations in Taiwan, which has the capacity of 1.44 kW. The simulation model is also validated by real experimental data and the close correlation between the simulated and experimental values for the water temperature has also been represented. The results indicate that Tainan in Taiwan is better than another location for the installation of the Photovoltaic thermal module. The electrical efficiency of the system was found to be 11.7-12.4 % whereas the thermal efficiency has the range 26.78-28.41 %.

Irem et al. [37] evaluated the effects of using various working fluids like mono nano fluid and hybrid nano fluid on the overall efficiency and performance of a PV thermal system compared to that of water. Using ANSYS, they numerically analyzed and compared the effects of different velocities at the inlet for base fluid or pure water, CuO+Fe/Water, and CuO/Water for cooling the solar cells in terms of temperature gain, thermal efficiency, cell temperature, electrical and total efficiency, and pressure drop. In order to determine the suitable volume concentration, the thermo-physical properties for working fluids up to 2% volume concentration were also studied. It's found that there is a positive impact on thermal efficiency for increasing fluid velocity but at the same time pressure drop is also increased. Comparing both with water under 2% concentration, the hybrid nano fluid showed much greater increase in both the electrical and thermal efficiency relative to mono nano fluid. However, hybrid nano fluid is also observed to have the highest pressure drop compared to other working fluids.

2.3 Review on combined Experimental and Numerical Research

Mourshed et al. [38] experimented and numerically analyzed a single pass hybrid PVT module with dual cooling system incorporating both water and air as coolants and evaluated its economic feasibility in Bangladesh. He included self-sustaining forced air circulation to improve PVT performances. The effects of water and air mass flow rates were also analyzed with varying solar irradiance. He found both electrical and thermal efficiency to increase with combined efficiency of 39.68%. In addition, mixing glycerin to water significantly increased overall efficiency to 45.76%

Bahaidarah et al. [39] both experimentally and numerically inspected the cooling effect by introducing a cooling panel which is supposed to work as a heat exchanger at the panel's rear surface. The setup was situated in Dhahran, Saudi-Arab. They presented that with active water cooling the temperature of the module decreased about 20%. Because of that the photovoltaic panel's electrical efficiency increased by 9%.

Khelifa et al. [40] performed a simulation on hybrid PVT collector using Ansys and obtained temperature distribution by employing air as a coolant, which results into cooling of the PV module. In this study, the variation of temperature in each cell of the PVT module is shown, from which it is observed that the cell temperature is lower causing both the electrical and thermal efficiency to increase. The coolant temperature found from the numerical calculation matches with the experimental result of heat transfer performance of a hybrid PVT (photovoltaic thermal) solar collector.

Strebkov et al. [41] developed a CFD model of PVT module which reveals the temperature and pressure contours for the water coolant for the varying coolant flow rate. The results for coolant temperature at the outlet were verified by the experimentation and relative errors were found to be no more than 1%. The temperature and pressure distribution of the coolant at a constant coolant flow rate (14.6 l/h) was shown based on the constant total insolation which was calculated from the inbuilt solar calculator.

Ionut et al. [42] developed a thermal model and validated the model based on experimental data to find a temperature distribution of a PV module located at varying distances relative to a roof wall along with the temperature and velocity distributions at the air channel exit. The numerical simulation was carried out by implementing the Galerkin finite element method, employing an implicit convective boundary condition. It's observed that distance from air inlet as well as the channel width affect both the

velocity and temperature. A good correlation was found between the experimental and stimulated results indicating a good accuracy for the model. Furthermore, the influence of two boundary layers (PV module, and roof wall) on the velocity and temperature was also studied.

Chapter 03: METHODOLOGY OF THE RESEARCH

3.1 Geometrical Model

The geometrical setup used for this study is a hybrid PV/T module where four different types of ribs were incorporated for four cases. The dimensions and parameters of the geometrical model were taken from the experimental work which was conducted by [24]. The entire construction is built in a wooden box. At the top of this wooden box PV collectors are set. Absorber plate is situated at the middle of the setup and eight copper tubes which act as water heat exchangers are set on top of that. Natural circulation occurs here because of the differential density between the water at inlet and outlet. Below the water heat exchangers (WHX) and absorber plate, 0.1m height air channel is introduced. On the opposite surface of the air channel four different ribbed surfaces plates (Flat, Square, Triangular, and Semicircular) of similar height are constructed. The absorber plate is made of steel. And for higher heat absorption both the absorber plate and the ribbed surfaces are painted black. The inner part of the wooden box is insulated. Figure 6 to Figure 9 presents the schematic diagram of the geometrical model with four different ribbed plates.

The major components of our geometrical model are PV panel, absorber plate, eight water heat exchangers, wooden box, insulation, air channel with different ribbed surfaces.

3.1.1 Dimensions of the components of the solar PVT panel

Thorough descriptions of each component are explained below:

<u>Solar PV Panel</u>
PV panels of Polycrystalline-Silicon (pc-Si) are incorporated in our study with 50 watts rating and the aperture area is 0.45m². The dimensions are specified as ($839 \times 537 \times 50$) mm.

<u>Wooden Box</u>
The entire setup is built in a wooden box having dimensions of (1000×670) mm.

Water Heat Exchanger (WHX)

For the natural circulation of water eight tubes were introduced. They are known as water heat exchangers. They are composed of copper. As copper has higher thermal conductivity compared to other accessible materials, it was selected to achieve high heat transfer. The diameter of each tube is 1.25 cm (½″).

Absorber Plate

The material of the absorber plate is specified as steel. It is painted black to upsurge the absorbency of heat. The thickness was considered negligible.

Ribbed Plate

Four different ribbed surfaces were introduced at the opposite of the air channel. The shapes are Flat, Square, Triangular and Semicircular. The ribbed surfaces are also painted black.

Insulation

Glass wool was introduced for insulation in the experimental setup, but we just specified that the outer surface of our computational domain has zero heat transfer rate.

3.1.2 Detailed Schematic Diagram according to the experimental setup
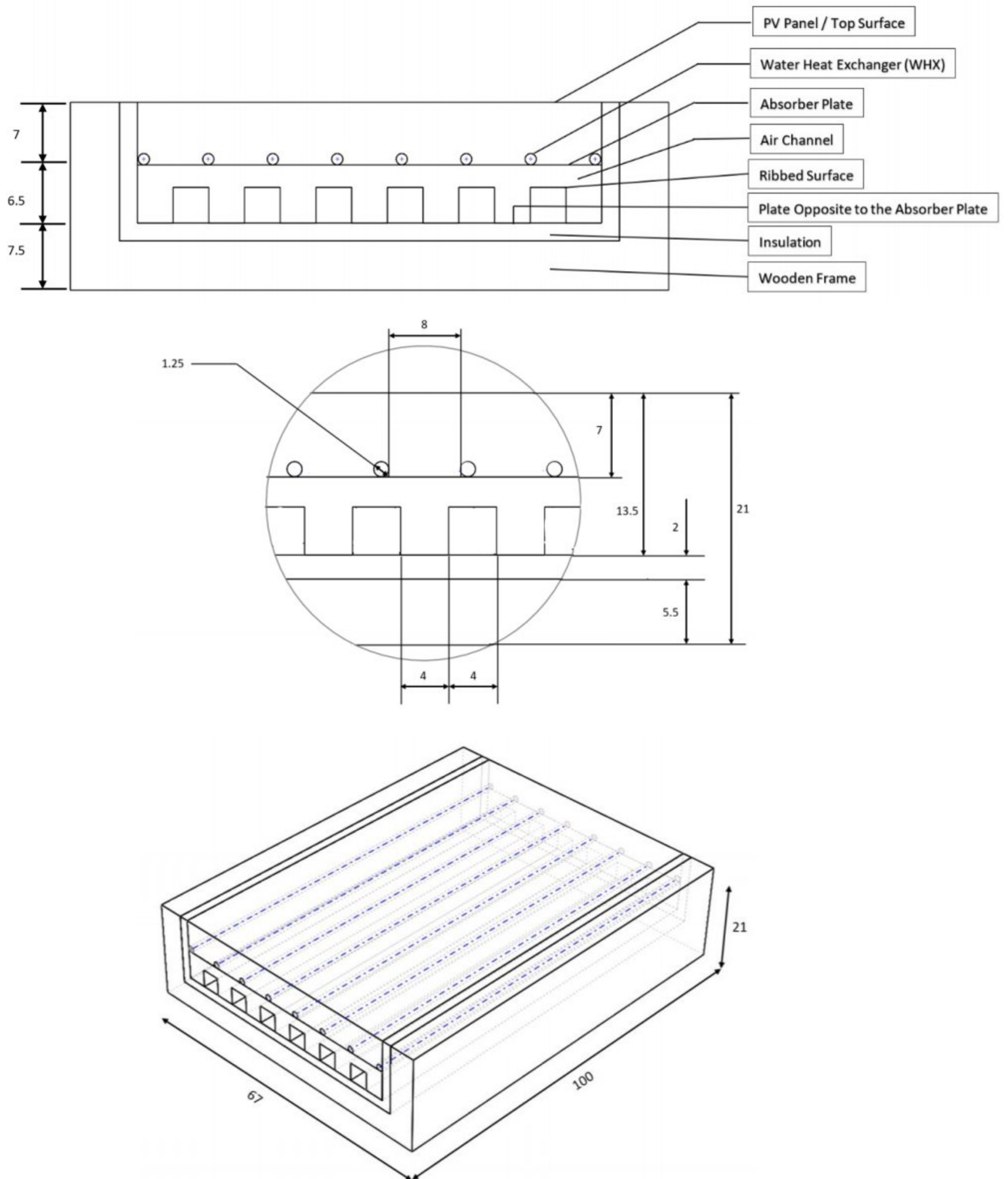
Figure 5: Detailed Schematic Diagram according to the experimental setup introducing rectangular ribs.

[All the dimensions are in centimeter]
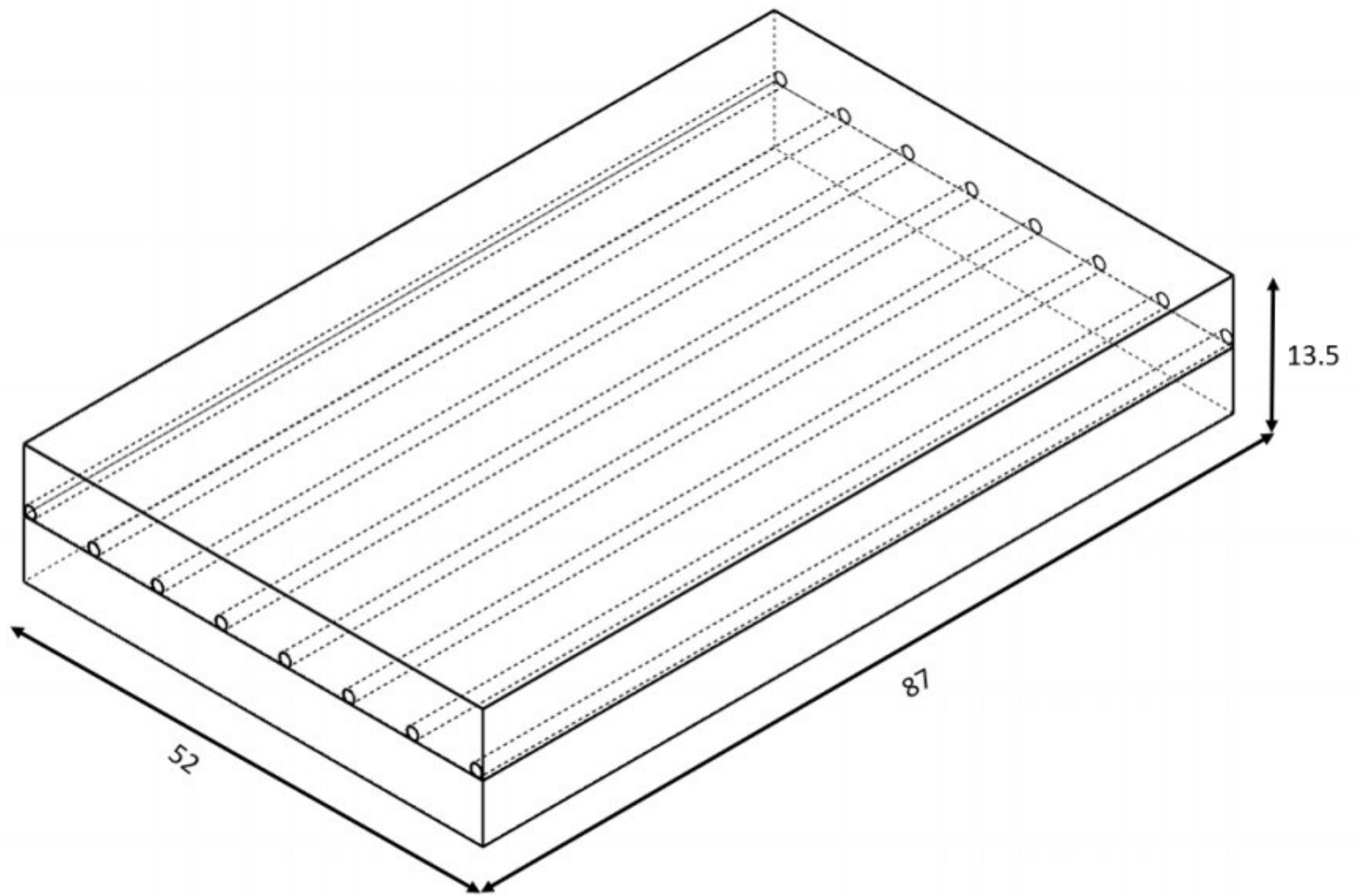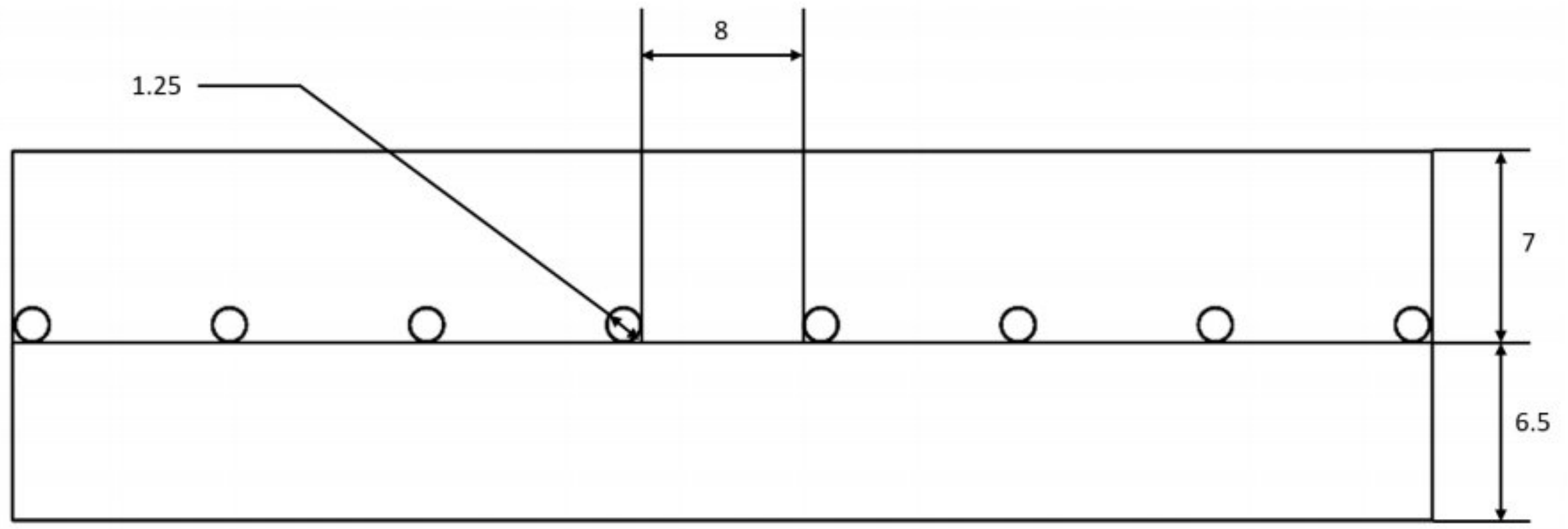
Figure 6: Detailed Schematic Diagram of the geometrical model introducing flat plate.

[Front View and Isometric View] [All the dimensions are in centimeter]
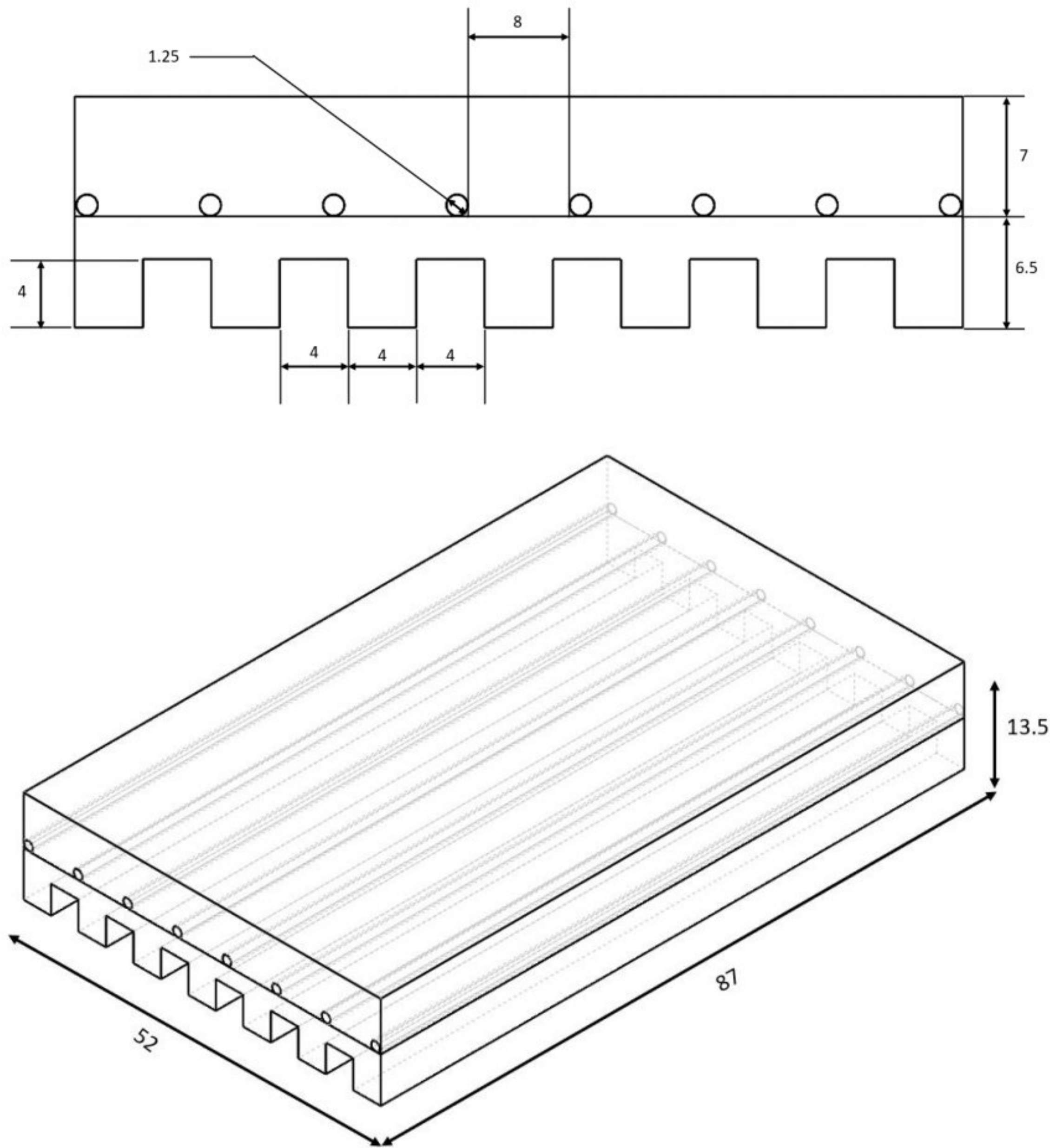
Figure 7: Detailed Schematic Diagram of the geometrical model introducing rectangular ribs.

[Front View and Isometric View] [All the dimensions are in centimeter]
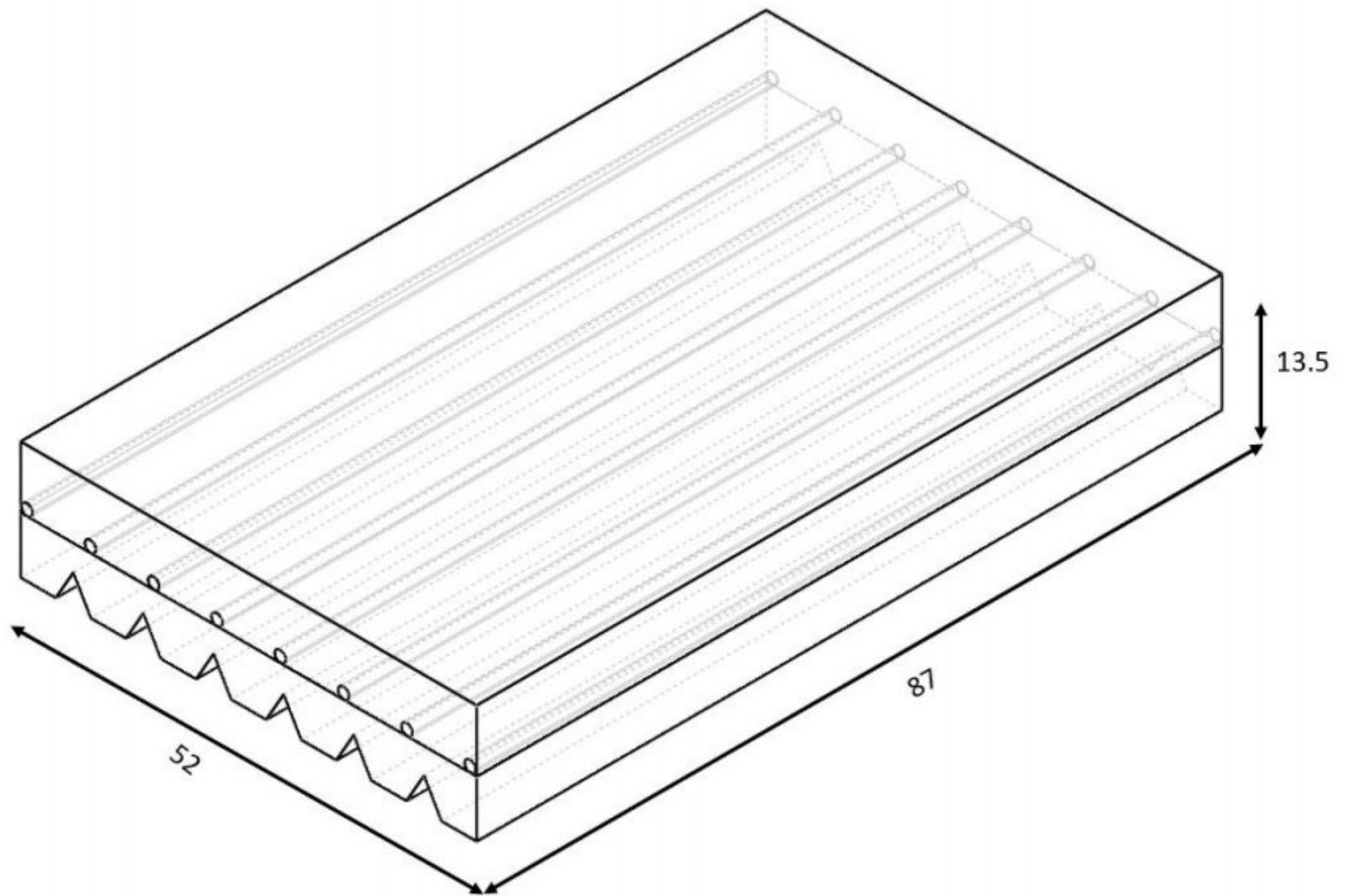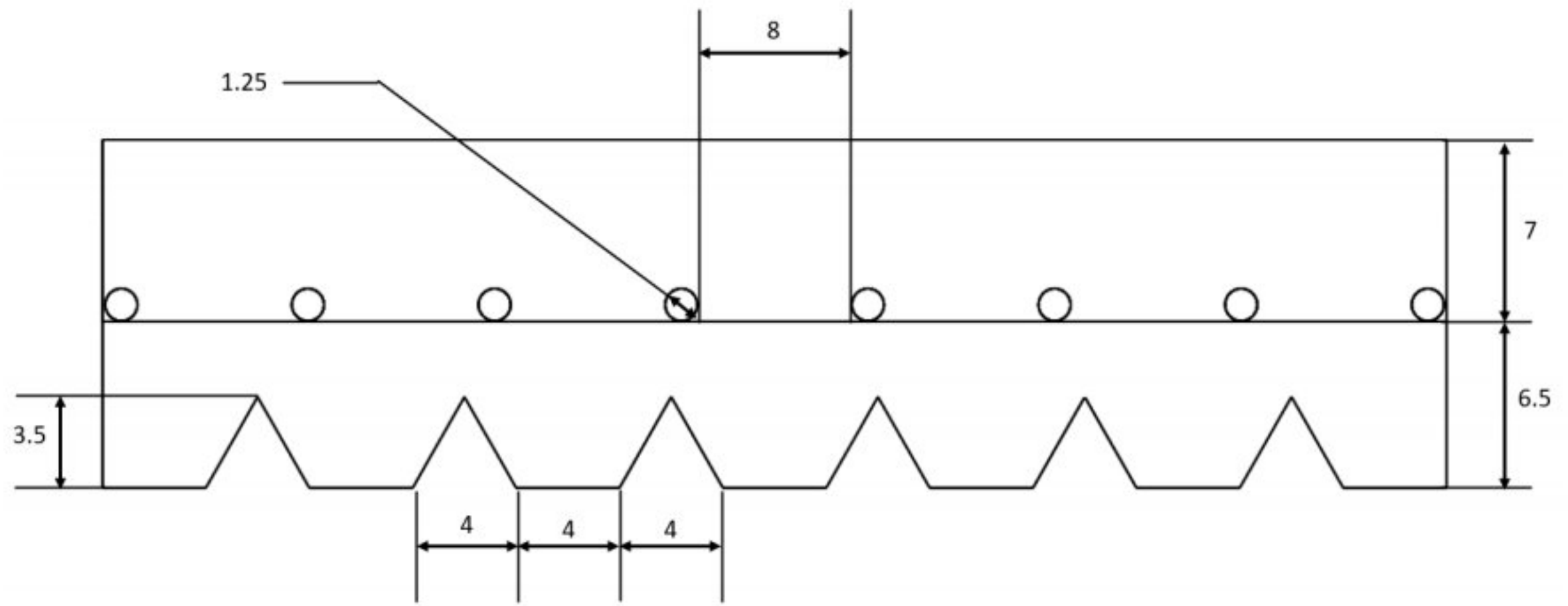
Figure 8: Detailed Schematic Diagram of the geometrical model introducing triangular ribs.

[Front View and Isometric View] [All the dimensions are in centimeter]
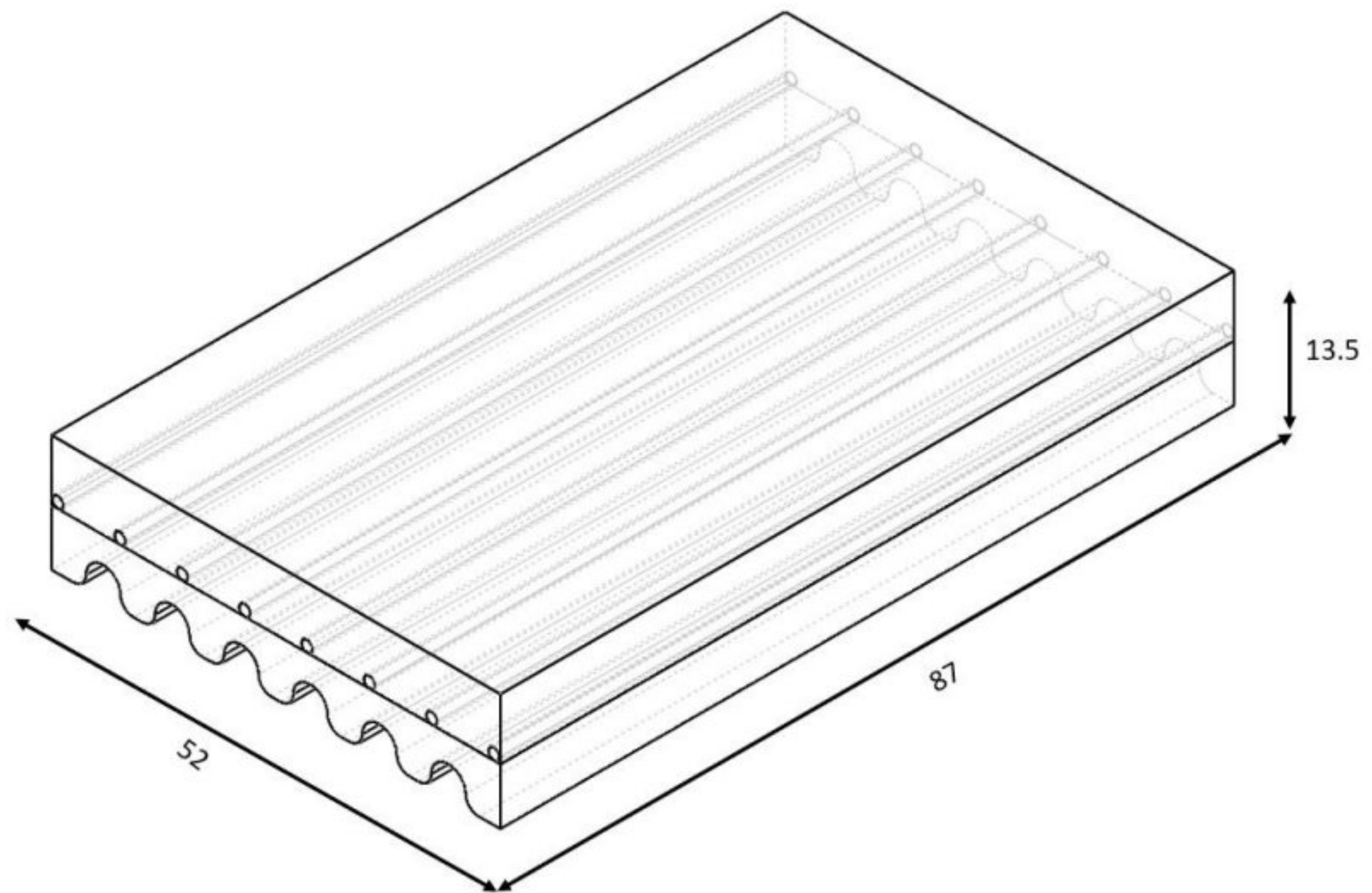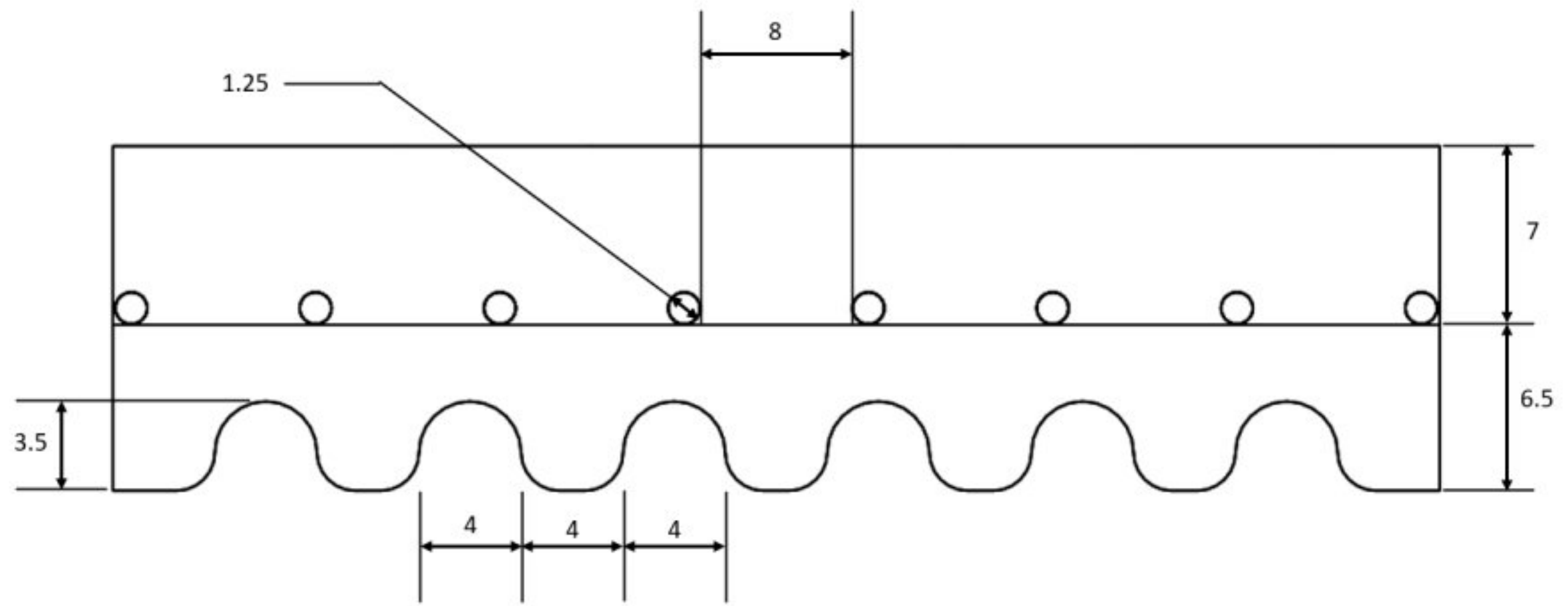
Figure 9: Detailed Schematic Diagram of the geometrical model introducing semicircular ribs.

[Front View and Isometric View] [All the dimensions are in centimeter]

3.1.3 Governing Equations

Mass Conservation Equation:

$$\frac{\partial \rho}{\partial t} + \nabla \cdot (\rho u) = 0$$

Continuity Equation:

$$\frac{\partial u}{\partial x} + \frac{\partial v}{\partial y} + \frac{\partial w}{\partial z} = 0$$

For the water flow inside the copper water heat exchangers, the momentum equations are: [Assumption: Incompressible Laminar Flow]

For Water flow in the x-direction:

$$u\frac{\partial u}{\partial x} + v\frac{\partial u}{\partial y} + w\frac{\partial u}{\partial z} = -\frac{1}{\rho_w}\frac{\partial P}{\partial x} + v_w\left(\frac{\partial^2 u}{\partial x^2} + \frac{\partial^2 u}{\partial y^2} + \frac{\partial^2 u}{\partial z^2}\right)$$

For Water flow in the y-direction:

$$u\frac{\partial v}{\partial x} + v\frac{\partial v}{\partial y} + w\frac{\partial v}{\partial z} = -\frac{1}{\rho_w}\frac{\partial P}{\partial y} + v_w\left(\frac{\partial^2 v}{\partial x^2} + \frac{\partial^2 v}{\partial y^2} + \frac{\partial^2 v}{\partial z^2}\right)$$

For Water flow in the z-direction:

$$u\frac{\partial w}{\partial x} + v\frac{\partial w}{\partial y} + w\frac{\partial w}{\partial z} = -\frac{1}{\rho_w}\frac{\partial P}{\partial z} + v_w\left(\frac{\partial^2 w}{\partial x^2} + \frac{\partial^2 w}{\partial y^2} + \frac{\partial^2 w}{\partial z^2}\right)$$

Energy Equation:

$$\rho C_p \frac{\partial T}{\partial t} + \rho c_p (u \cdot \nabla)T = -(\nabla \cdot \dot{q}) + \tau S - \frac{T}{\rho}\left(\frac{\partial \rho}{\partial t}\right)_P \left[\frac{\partial p}{\partial t}(u \cdot \nabla)p\right] + \dot{q}_v$$

3.1.4 Mathematical Equations

The electrical efficiency of the PV Panel can be calculated using this following equation:

$$\eta_{pv} = \frac{p_{\max}}{A_a G} = \frac{I_{max} v_{max}}{A_a G}$$

The thermal efficiency can be calculated from this equation:

$$\eta_{th} = \frac{\dot{m} C_p (T_{out} - T_{in})}{A_a G}$$

For the projected area, the heat energy absorbed 1 hour:

$$Q_{ab} = m C_p \Delta T_\omega$$

For the projected area, the solar radiation received in 1 hour:

$$I = G \times A_a \times 3600 \ (joule)$$

3.1.5 Considered Cases

The main purpose of our study is to determine the water outlet temperature of the water heat exchanger.
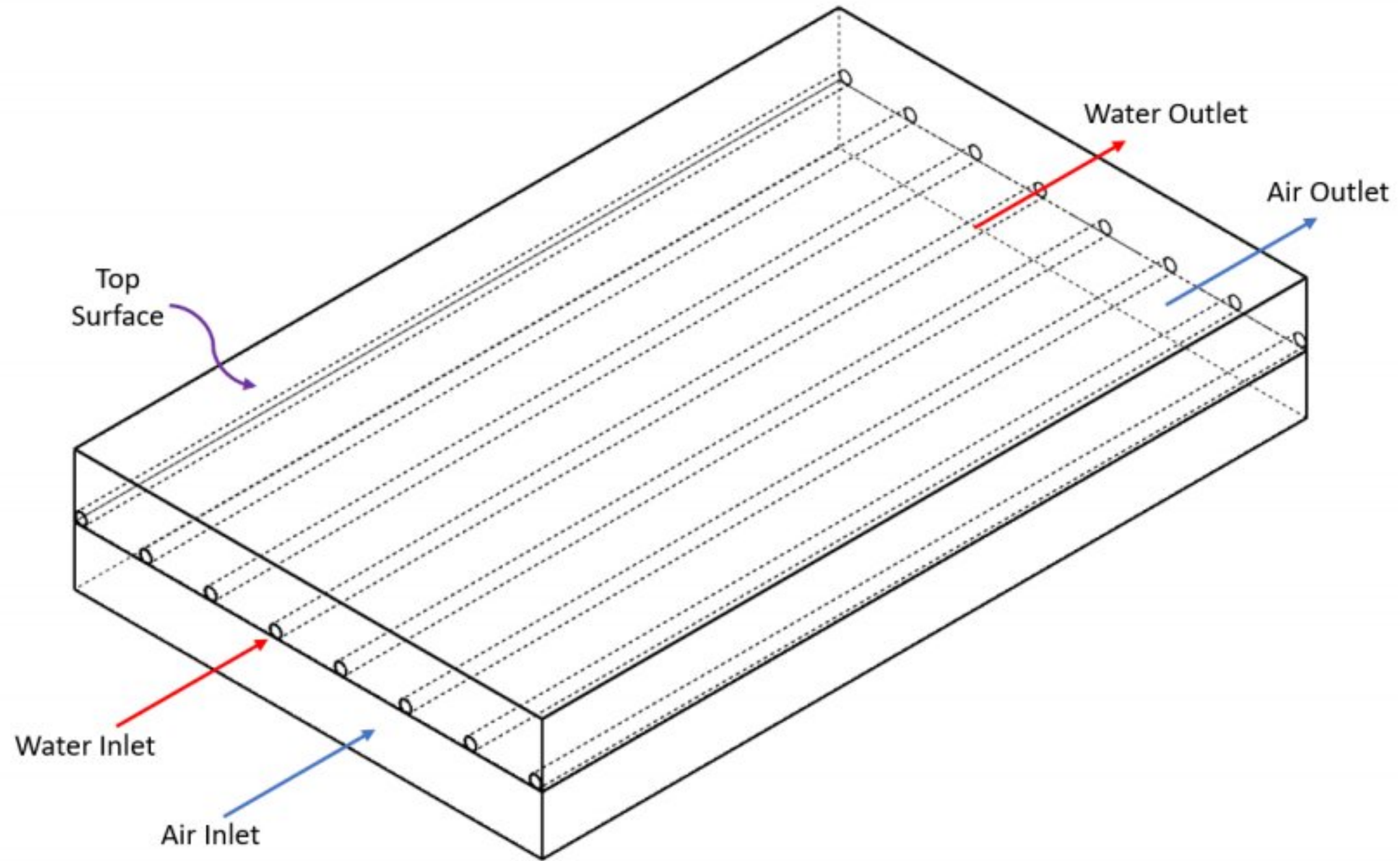
Figure 10: Hybrid PV/T Panel showing the inlet-outlet port of the water heat exchanger - WHX and air channel. [Flat Plate]

Table 1: All the considered cases for the Hybrid PV/T panel based on water and air velocity.

Case no	Geometrical Configuration	Water Velocity	Air Velocity
1	Flat plate	Constant	Constant
		Constant	Variable
		Variable	Constant
2	Rectangular ribbed plate	Constant	Constant
3	Semicircular ribbed plate	Constant	Constant
4	Triangular ribbed plate	Constant	Constant

In our geometrical models, four different types of ribbed surfaces (Flat plate, Rectangular ribs, Triangular ribs and Semicircular ribs) are incorporated. For each of the geometry we have considered the water and the air velocity constant. We have simulated six times for each geometry from 10:30 am to 1:00 pm with an interval of 30 minutes. All the values were taken from the reference paper[24]. The water velocity and the air velocity were also assumed based on the experimental conditions. By considering these conditions we procced to validate the water outlet temperature of the water heat exchanger with the reference paper.

Table 2: Water inlet temperature of all the considered cases for the Hybrid PV/T panel based on specified time

	10:30 am	11:00 am	11:30 am	12:00 pm	12:30 pm	1:00 pm
Flat plate	306 K	307.5 K	309 K	310 K	311 K	311.5 K
Rectangular ribs	308 K	309 K	310 K	311 K	312 K	312.5 K
Semicircular ribs	310 K	311 K	312 K	313.8 K	315 K	315.5 K
Triangular ribs	311 K	312 K	313 K	313.8 K	314 K	314.5 K

Every 30 mins interval we have provided the water inlet temperature in our setup to achieve our required water outlet temperature of the water heat exchangers. Total six times were taken into consideration which are 10:30 am, 11:00 am, 11:30 am, 12:00 pm, 12:30 pm and 1:00 pm respectively. We have simulated for these six individual times for each geometrical configuration. These inlet water conditions were taken from the experimental work which was conducted on February and March, 2010 [24].

Table 3: Considered cases for variable water velocity for flat plate

	Case 1		Case 2	
	Water Velocity, m/s	Air Velocity, m/s	Water Velocity, m/s	Air Velocity, m/s
Flat Plate	0.005			0.25
	0.006			0.3
	0.007	Constant	Constant	0.4
	0.009			0.8
	0.01			1
	0.02			1.1
	0.04			-

To find out the novelty of our study we further investigated the changing effect of water outlet temperature by changing the water velocity several times and considering the air velocity as constant. We also tried to change the air velocity while keeping the water velocity constant to check the change. These two conditions were only considered for flat plate.

3.2 Numerical Model

The study has been conducted with the help of ANSYS 2020 R1 Software package. The work also has been verified and validated by some experimental and numerical investigations that were previously done. The numerical methodology and approach will be described in detail in this chapter. But in order to execute the solution by Ansys solver, proper boundary conditions must be specified. Grid independency test should also be done to select the suitable mesh size throughout the entire simulations. It is also very important to check whether our solution is converged by monitoring the residuals based on preset criteria or adding additional convergence criterion.

3.2.1 Numerical Approach and Assumptions

- ✓ All geometries are designed using SOLIDWORKS 2019. And then the files were imported to the Ansys geometry section. Further modifications have been done in the Space Claim on the geometry, and the topology was shared so that the mesh to be generated on the intersecting surfaces could match properly.

- ✓ The Origin is considered to be at the inlet position for all four geometries. The gravitational force acts along the negative Y direction. On the other hand, the fluid flows through inlet along the positive z direction.

- ✓ Ansys meshing software was used for meshing. The grids are generated using ANSYS Mechanical. The mesh size was decided based on the mesh independency test. The grid independency test is performed to inspect the mesh quality and suitability. In order to ensure better mesh quality, the orthogonal quality must be higher and the skewness should be lower.

- ✓ ANSYS fluent solver was used for achieving the solution of the simulation.

- ✓ Pressure-based Solver, Absolute velocity formulation and Steady or time independent setup were selected in the Ansys fluent platform.

- ✓ The governing equations are solved to make sure for each control volume, the mass, momentum and energy is conserved in order to produce the flow field in PV Modules.

- ✓ Convergence is achieved when all the solution residuals fall under a preset-criteria. In this case convergence is obtained while all the residues are below 1×10^{-6} for the computational domain, which was the predefined criteria.

- ✓ Viscous laminar model was selected as the model for analysis and energy was enabled. Considering the Reynolds number will be much lower due to the lesser velocity of the water, laminar model was chosen.

- ✓ No slip boundary conditions are applied on the stationary walls.

- ✓ Coupled solver was used as the solution method scheme for pressure velocity coupling.

- ✓ Second order upwind schemes were chosen for both momentum and energy.

- ✓ The underrelaxation factors were adjusted properly for the solution. If the convergence is not reached, the underrelaxation factors must be reduced since this is a pressure-based solver. If this was a density-based solver, we would have to decrease the Courant number to approach closer to the convergence.

3.2.2 Boundary Conditions

The boundary conditions that were given to ANSYS are mostly taken from the experimental setup of the reference paper.

According to the cases that have been considered earlier, for all four geometries the air velocity and water velocity were constant. The temperature for water inlet, air inlet and PV panel were varying due to the intensity of solar radiation and atmospheric changes. And these variable values were also taken from the plotted graphs from the experiment of reference paper. [24]

Some stationary surfaces of the physical domain were specified as walls. No slip boundary condition has been implemented on the walls.

It's also very crucial to assign the materials for different components of the geometry. Since different materials have different properties such as thermal conductivity, heat capacity etc., this will have adverse effect on the overall heat transfer.

The values given as boundary conditions are mentioned below:

Air Velocity: 1 m/s

Air Inlet Temperature: Time dependent Variable (Taken from the reference paper) [24]

Water Velocity: 0.007 m/s

Water Inlet Temperature: Time dependent Variable (Taken from the reference paper) [24]

PV Panel: Time dependent Variable (Taken from the reference paper) [24]

Walls:

- Top Surface (PV Panel)

- Mid Surface (Absorber Plate)

- Water Pipes (Water heat exchanger)

Table 4: Materials and Properties for different components

Components	Material	Parameter	Values
Absorber plate (Mid Surface)	Steel	ρ	8030
		C_p	502.48
		k	16.27
PV Panel (Top Surface)	Polycrystalline Silicon	ρ	2330
		C_p	703.38
		k	149
Water Pipes	Copper	ρ	8978
		C_p	381
		k	387.6
Coolant	Water	ρ	998.2
		C_p	4182
		k	0.6
	Air	ρ	1.225
		C_p	1006.43
		k	0.0242

3.2.3 Mesh Independency or Grid Independency Test

Grid independency test is basically done to inspect mesh quality and find the suitable mesh for obtaining the desired solution, by trading off between two factors; the solution accuracy and computational time. [43] The more refined the mesh is, the more the solution accuracy but the more it will take time to reach the solution convergence. However, we want to ensure as much as solution accuracy reducing the computational time as much as possible since we have so many cases to run simulations for.

Grid independency for Flat plate with certain Boundary Conditions:

Water Inlet Temperature: 311.5 K

Water Velocity: 0.007 m/s

Air Inlet Temperature: 309 K

Air Velocity: 1 m/s

The expected result at the water outlet must be 312 Kelvin, according to the reference paper. [24]

Four sets of grids were generated using elements with 1119152 nodes, 912730 nodes, 437700 nodes, and 333056 nodes. The results for various grid sizes are compared and it is evident from the table, that the water outlet temperatures for grid size 4.5 and 5 are closest to the value 312K, which was taken from the reference paper. If we calculate the percentage of error with respect to grid size 5 and compare the values, it is observed that the percentage of error between these two grid sizes (4.5, and 5) are the lowest. Therefore, grid size 5 has been chosen as the constant grid size throughout the simulations to reduce the computational time maintaining a decent accuracy of the solution for numerical calculation. [44]

Table 5: Grid Independency test for four sets of grid sizes

Grid Size (mm)	Nodes	Element no.	Water Outlet temperature (K)	Percentage of Error (%)
4.5	1119152	1085625	311.978	0.0147
5	912730	883376	311.932	-
8	437700	423756	311.843	0.0285
10	333056	323723	311.808	0.0397
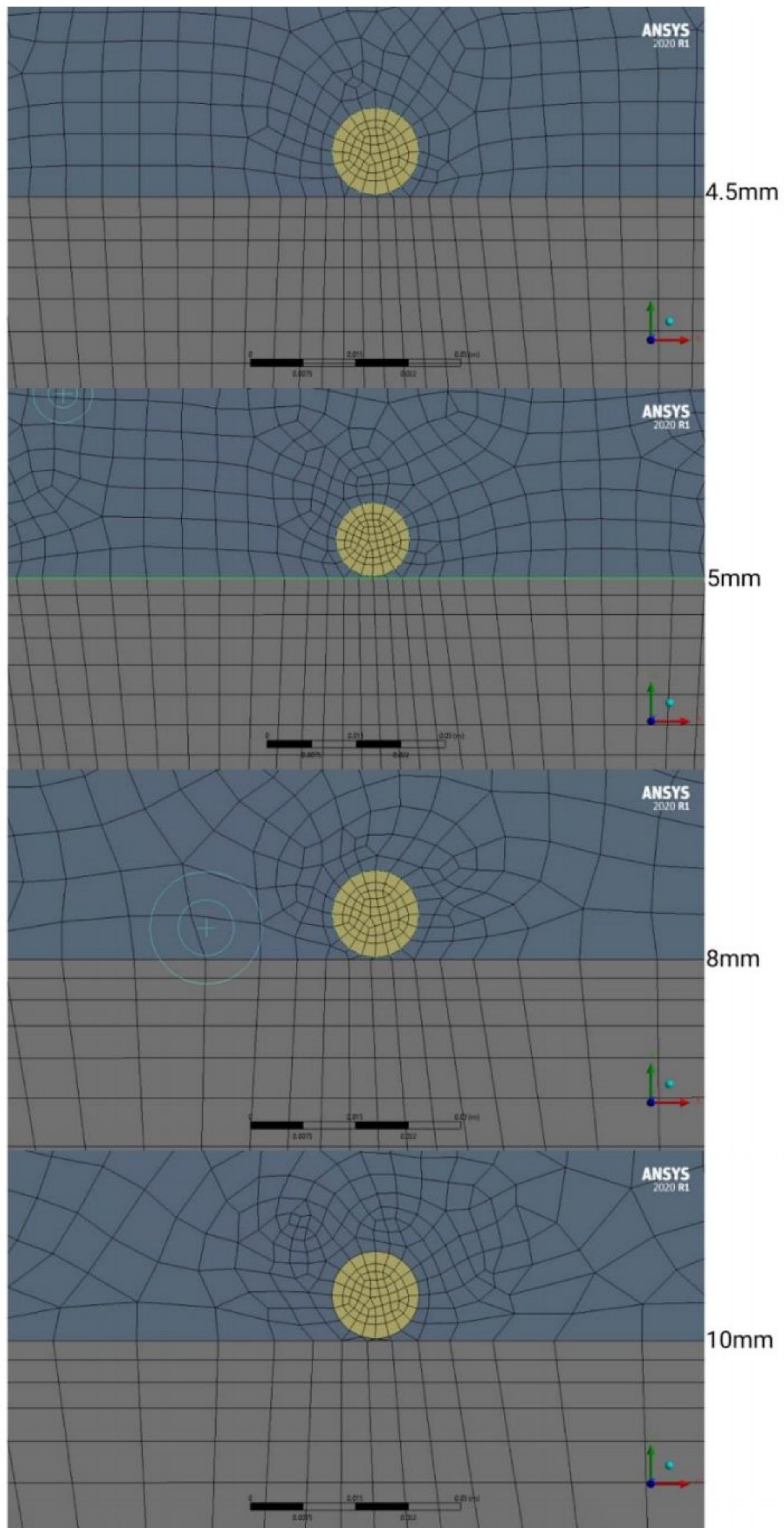
Figure 11: Evolution of the generated mesh depending on the four grid sizes

3.2.4 Solution Parameters

There are different solution methods for pressure velocity coupling, based on the various algorithms to obtain the solution to a certain problem. SIMPLE, PISO, COUPLED schemes are applicable to only pressure-based solver. Since our work uses a pressure-based solver, we've chosen COUPLED scheme. Only the coupled scheme uses the pressure based coupled algorithm, whereas other schemes use the pressure based segregated algorithm. Since this scheme offers the tendency to obtain more efficient and robust single-phase execution in case of steady state models, we've chosen COUPLED as our solution method for all of the cases through the simulations. The spatial discretization methods for gradient, pressure, momentum and energy have been selected based on the amount of accuracy is required and how much cost and time can be tolerated for computation. Since the second order pressure scheme is the best when there is no stability issue, second order method has been selected for pressure. Furthermore, the second-order upwind has much more accuracy than the 1st order one despite of having stability issues. Therefore, we've selected second order upwind scheme for both the momentum and energy solution methods.

As for the underrelaxation factors, we've run the simulations starting with defaults. In case of instability of the solution, the underrelaxation factors have been reduced to 0.25 as this is a pressure-based solver. The pseudo transient explicit relaxation factors for pressure and momentum are set to be 0.5, for density and body forces are set to be 1, and for energy 0.75 initial by default for most of the cases. Whenever there was a stability problem, each of the Relaxation factors were set to be 0.25.

3.2.5 Convergence Criterion

Any numerical model should be convergent only if a set of model solutions with continuously more refined solution domains tends towards a fixed value. In order to reach the convergence criterion, the set of model equations must converge to the solution of continuous equations governing the physical model for our study.

The absolute criteria have been preset to be 1×10^{-6} for all the solution residuals. However, in reality even if all these residuals fall below the predefined number, it doesn't necessarily mean the solution variable will stop changing. Therefore, in order

to be thorough, the behavior of the solution variables must be observed as the solver iterates. In this case, total heat transfer rate is defined in as one such solution variable, which will provide good indication of whether the heat is conserved. Under the monitors, in the convergence conditions section, additional convergence criterion can be added. After adding the report definition for total heat transfer rate, ignoring iterations before 20 and using 20 iterations, setting stop criterion to the default value of 0.001, the solution is initialized, and the calculation is run. Upon the completion of the calculation, it's observed that the solution for the report definition total heat transfer rate has been converged. Since this solution variable has stabilized, the solution has reached a considerable accuracy, which is also evident from the figure.
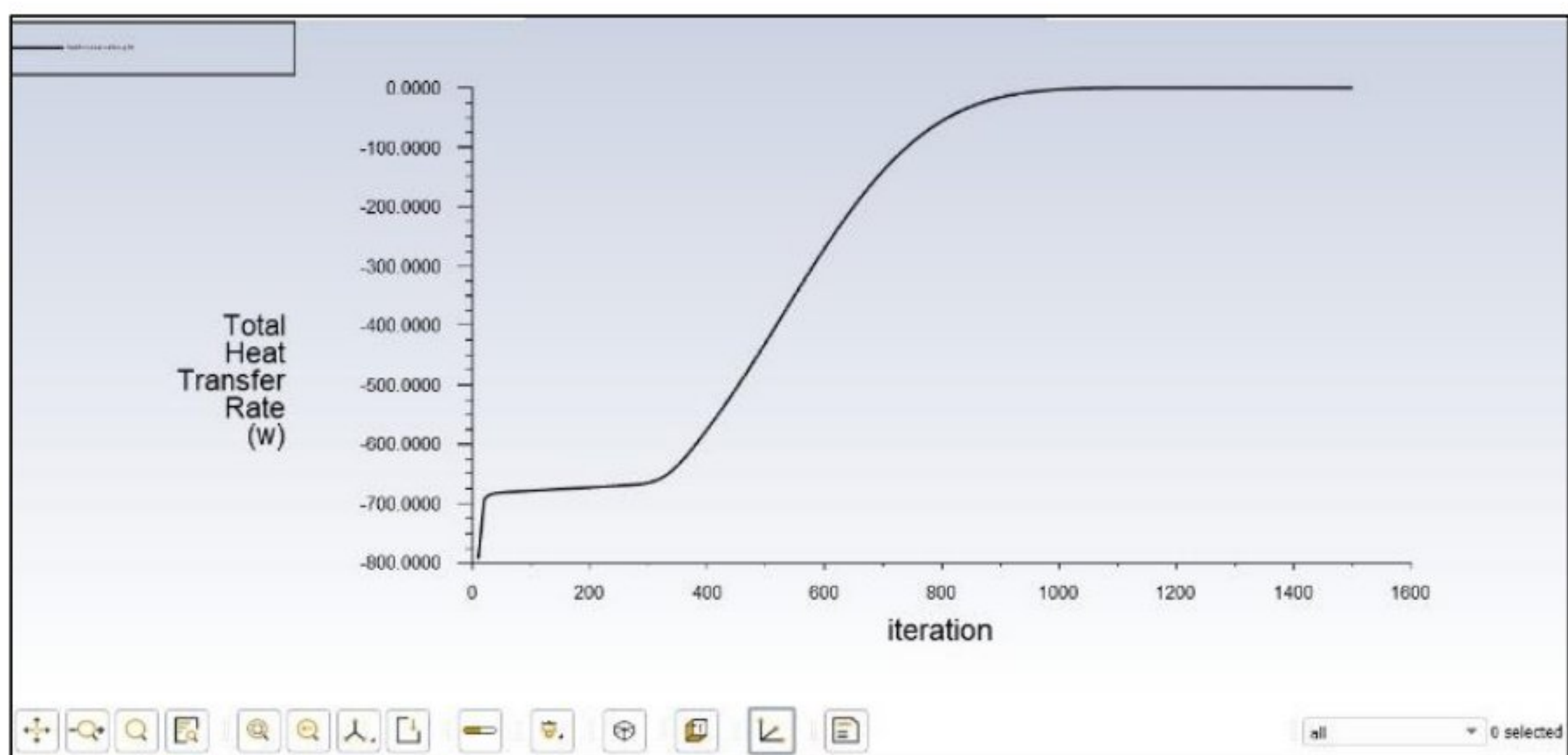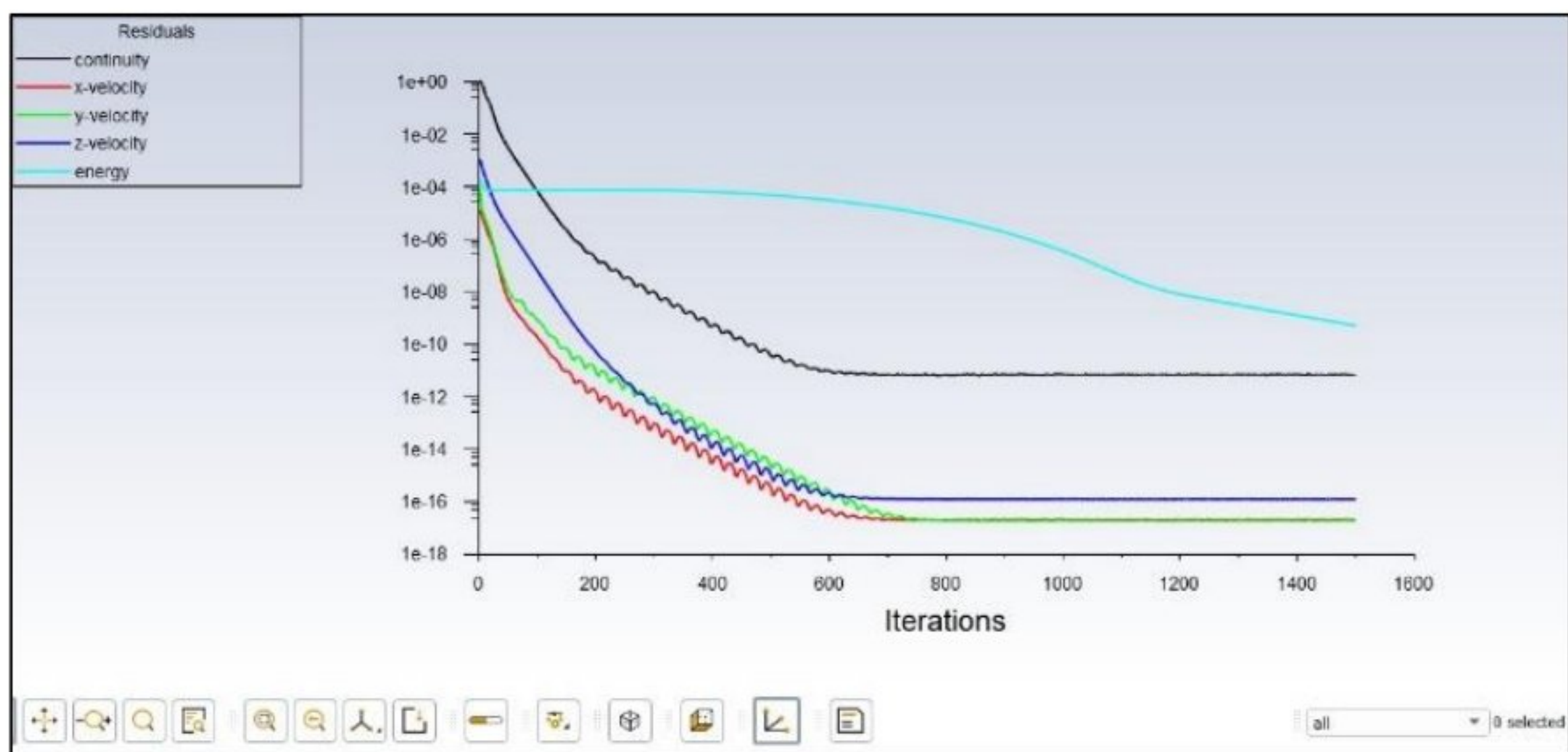
Figure 12: Checking for Convergence Criterion

Chapter 04: RESULT ANALYSIS AND DISCUSSION

4.1 Numerical Validation and Comparison
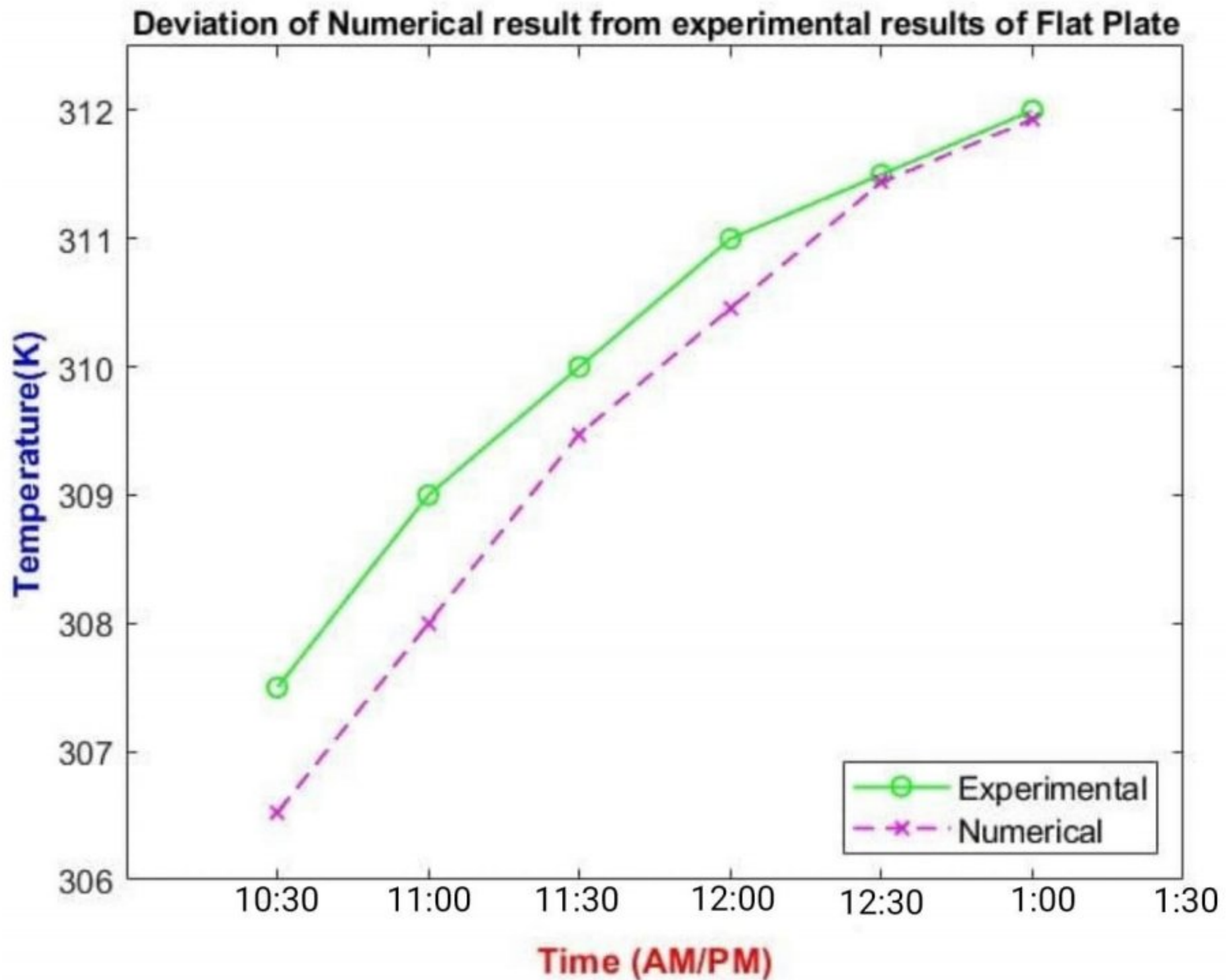
Figure 13: The comparative plots between the Numerical results and Experimental results in case of Flat Plate.[24]

This is the graph that was plotted by MATLAB from the results of ANSYS simulation. Here, the geometry with flat plate shows almost similar trends as the water outlet temperatures of the experiment.

At 10:30 am the difference of water outlet temperature between the experimental and numerical data was maximum. From 10:30 am to 12:00 pm, certain difference between the two values was observed. But as we can see at 12:30 pm and 1:00 pm, the error is at lowest point. Overall, the water outlet temperatures of WHXs taken from our numerical simulation is in acceptable range.
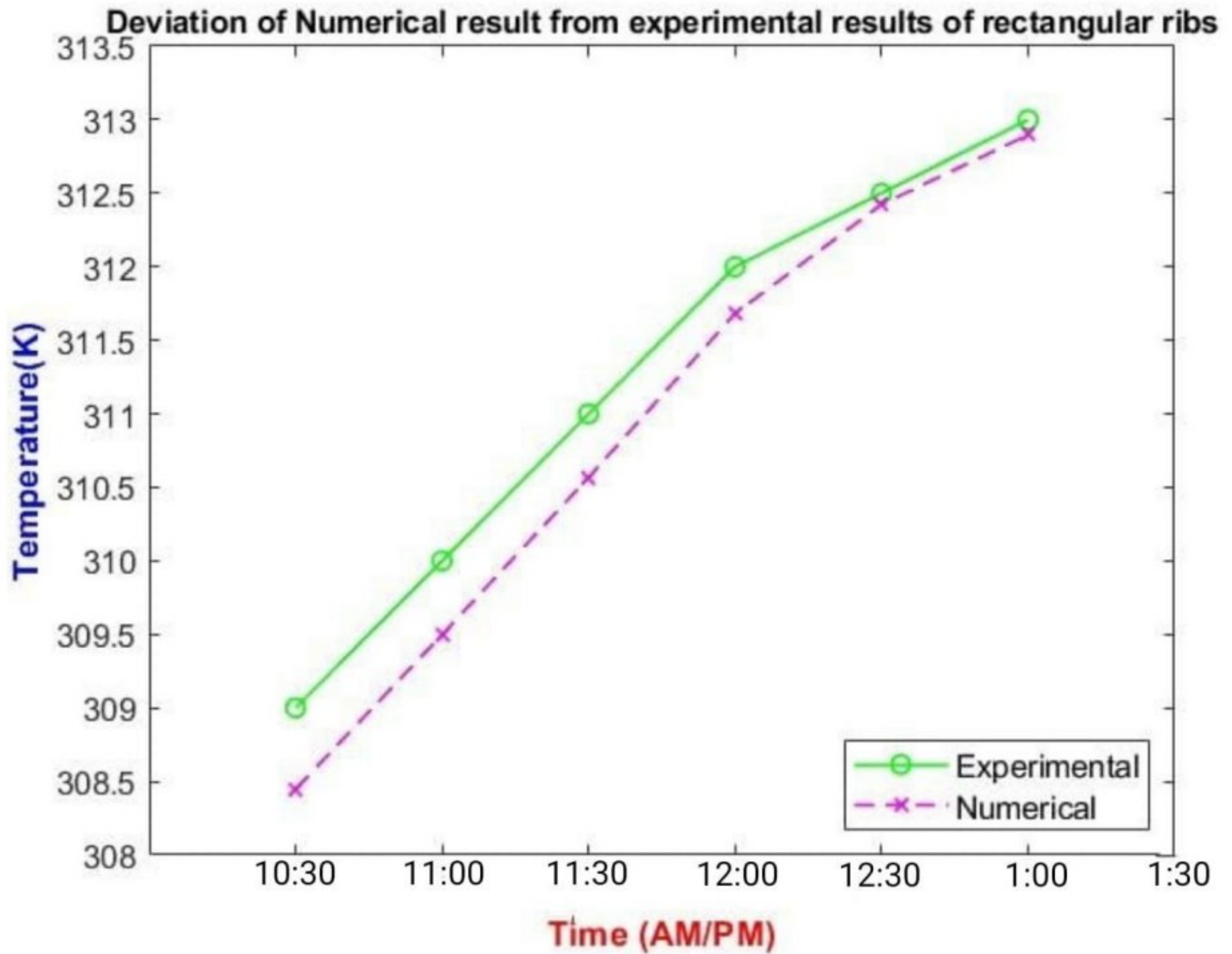
Figure 14: The comparative plots between the Numerical results and Experimental results in case of Rectangular Ribs.[24]

This graph was also plotted by MATLAB from the outcomes of our ANSYS simulation. From the graph we can observe that the geometry with rectangular surfaces shows almost same trends as the water outlet temperatures of the experimental results.

During 10:30 am the variance of water outlet temperature of the copper tubes between the experimental and numerical data was maximum. From 10:30 am to 12:00 pm, certain variance between the two values was detected. Nevertheless, as we can see at 12:30 pm and 1:00 pm, the difference is at bottommost point. In general, the water outlet temperatures of WHXs from the numerical simulation is in satisfactory range.
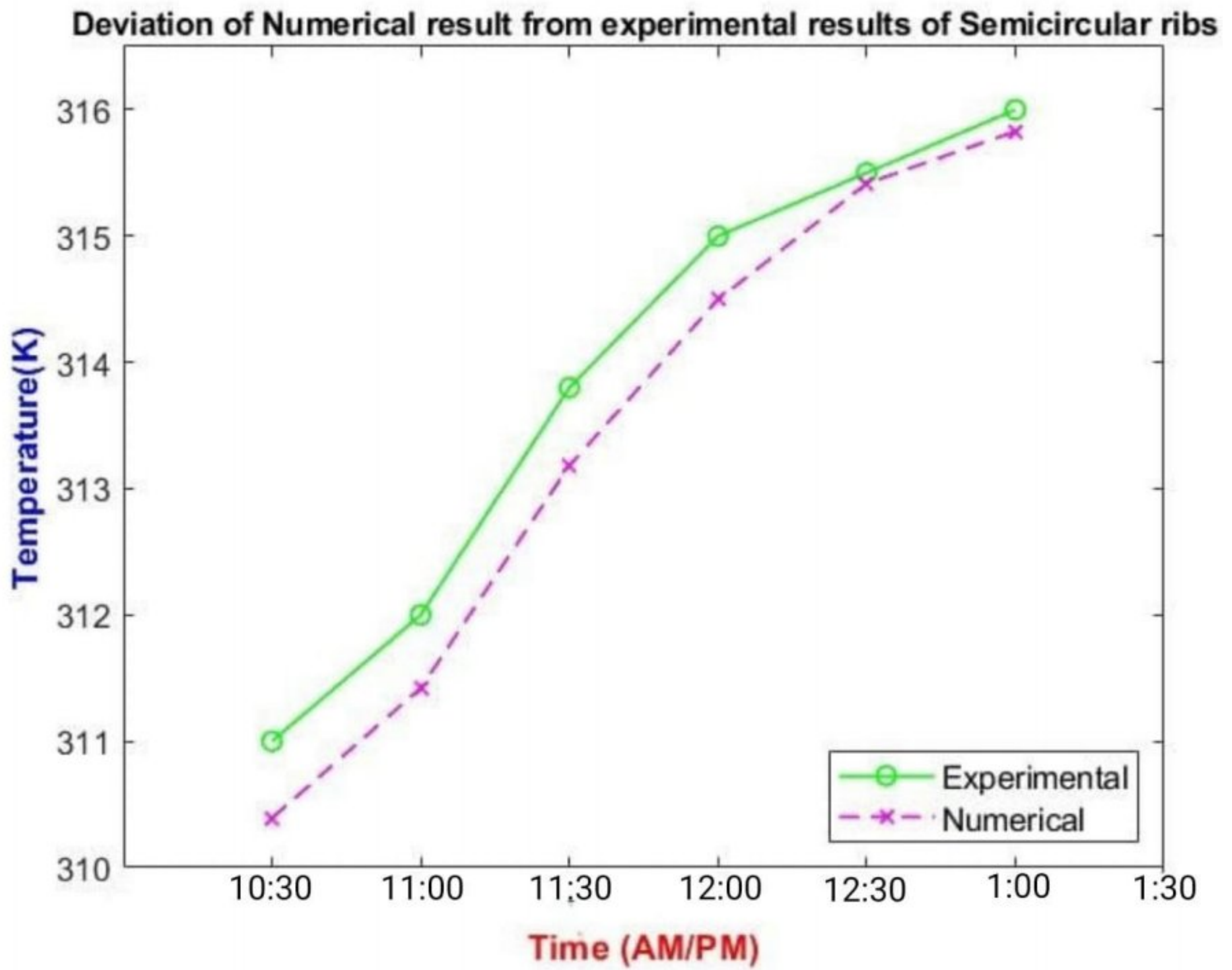
Figure 15: The comparative plots between the Numerical results and Experimental results in case of Semicircular Ribs.[24]

Above graph was plotted by MATLAB from the results after the completion of the ANSYS simulation. Here, the geometrical configuration with semicircular surfaces displays nearly similar trends as the water outlet temperatures of the experiment. As we can see at 12:30 pm and 1:00 pm, the error is at lowest point. Overall, the water outlet temperatures of WHXs collected from our numerical simulation is in suitable range.
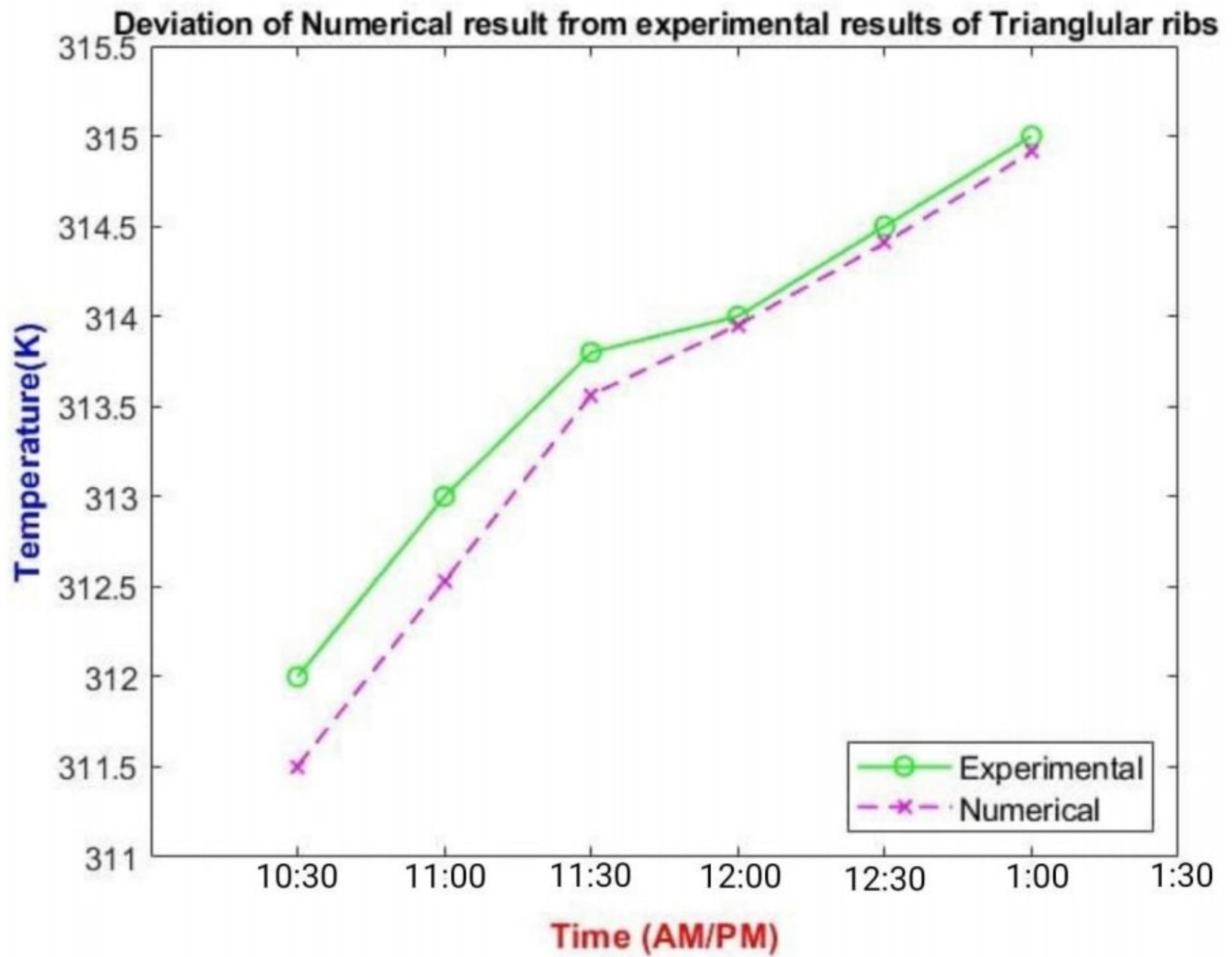
Figure 16: The comparative plots between the Numerical results and Experimental results in case of Triangular Ribs.

This one is also plotted by MATLAB. And the numerical results are almost similar to the experimental one. In general, we can observe that the water outlet temperatures of WHXs from the numerical simulation is in satisfactory range.
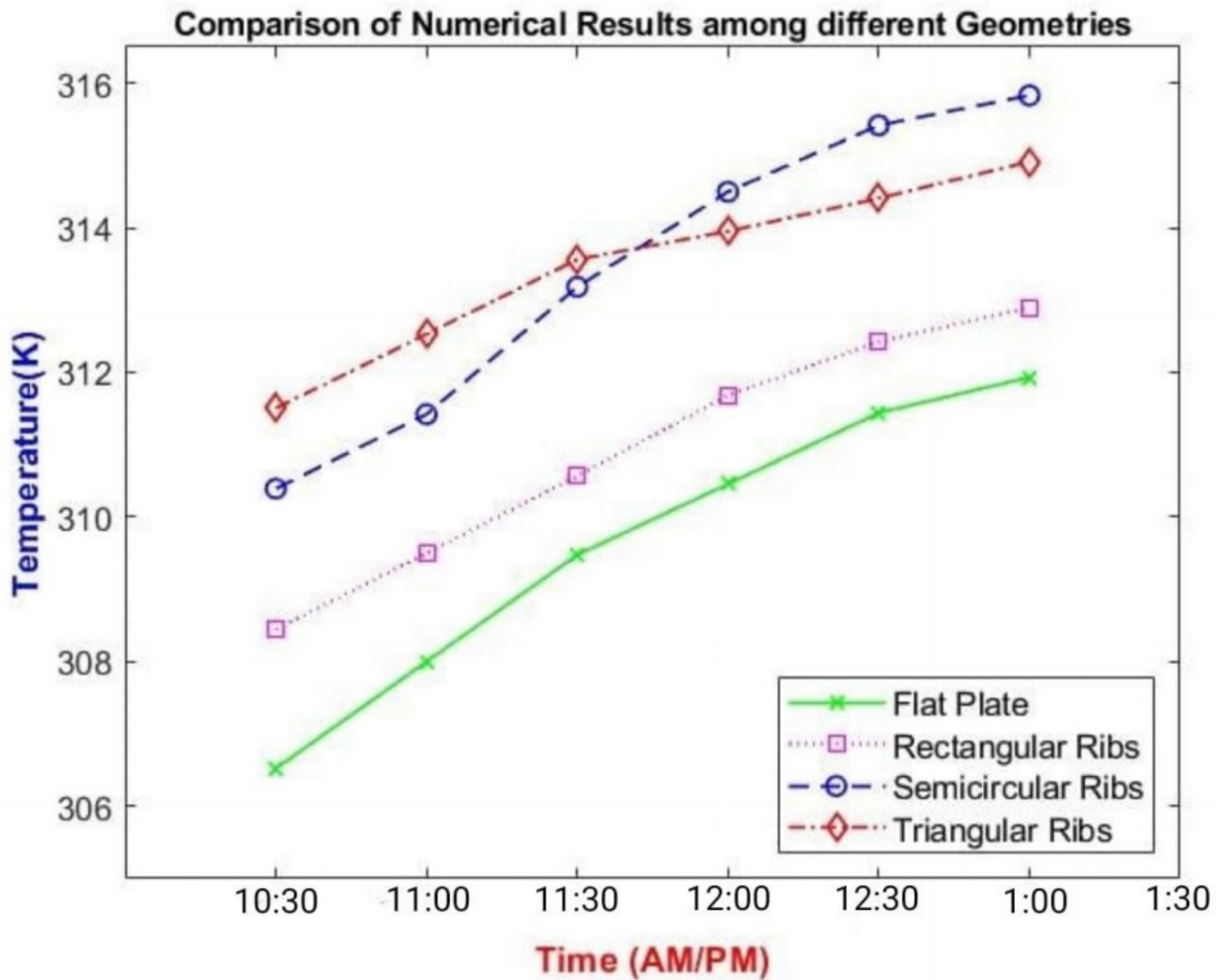
Figure 17: Comparison of Numerical results among all four different geometries

If we compare the numerical results, the water outlet temperatures of the geometries with semicircular and triangular ribs are significantly higher compared to the other geometries. Thus, they are more effective for extracting heat through water. Therefore, for these two geometrical configurations, the PV panel will be effectively cooled resulting in optimum thermal and electrical efficiency.
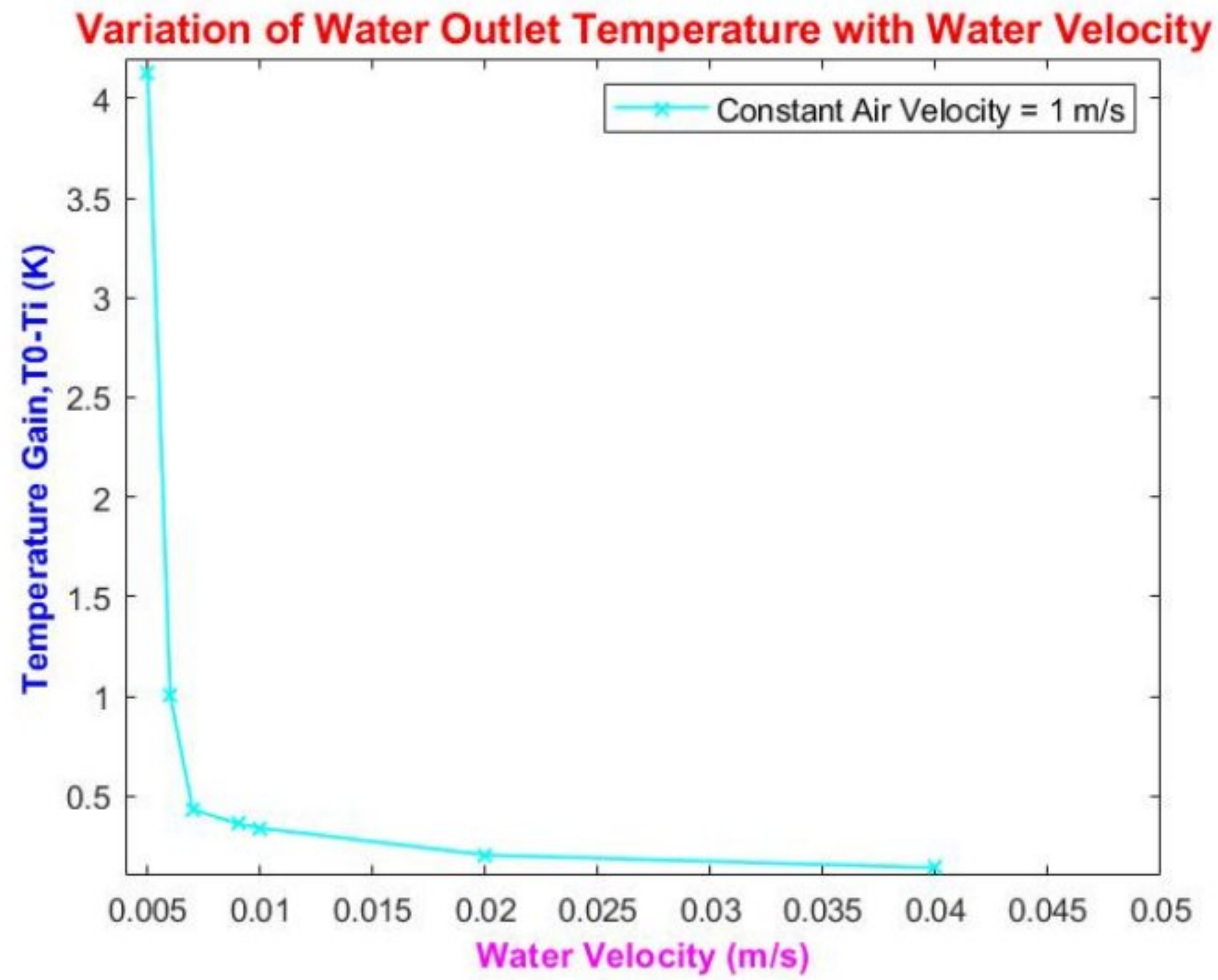
Figure 18: The trend for Water Outlet Temperatures with varying Water velocity
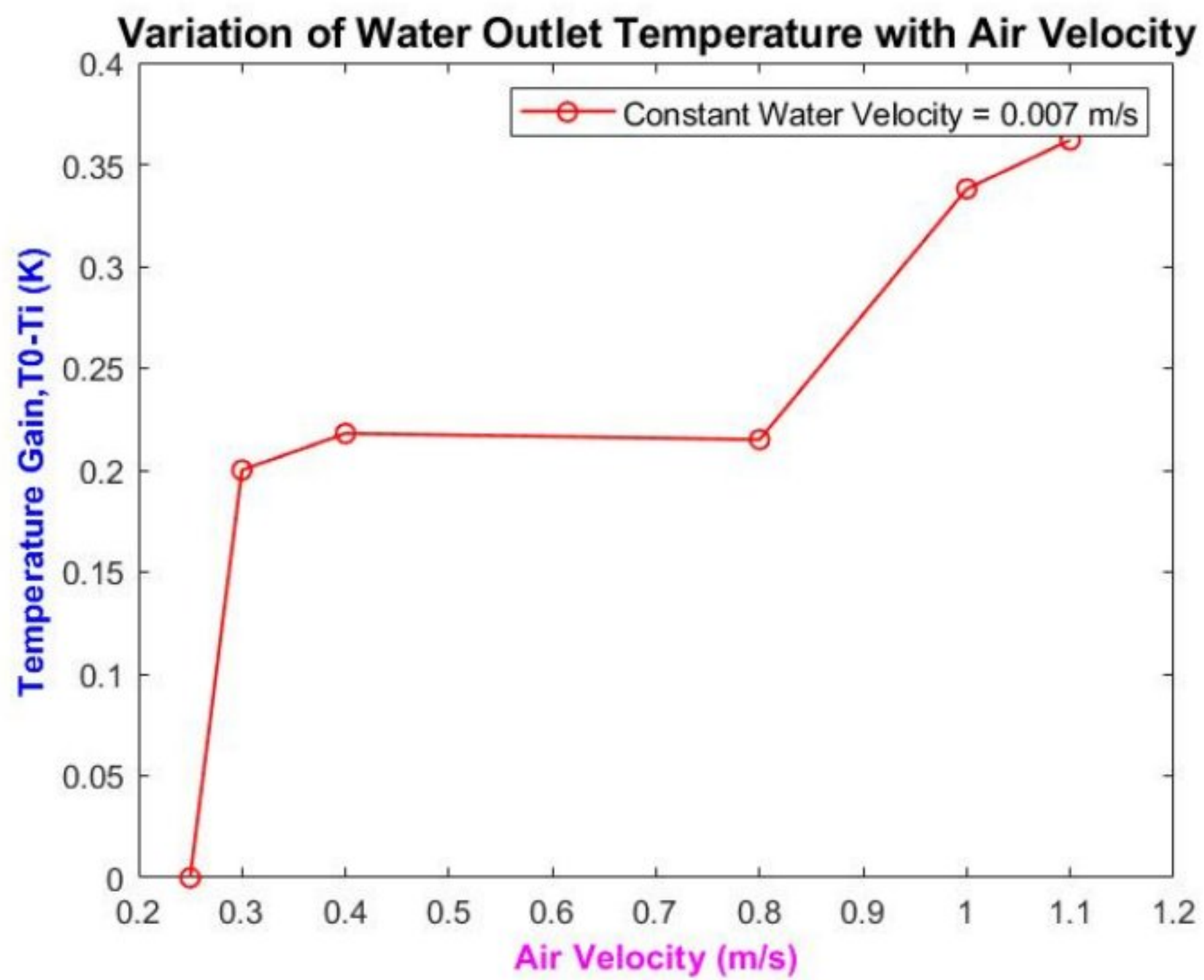
Figure 19: The trend for Water Outlet Temperatures with varying Air velocity

If we study the effects of water and air velocities on the temperature gain for water based on the results of our simulation, from these two trends it can be concluded that temperature gain enhances with increasing air velocity and decreasing water velocity. Therefore, to achieve greater thermal performance, we should thrive to attain higher air velocity and reduce the water velocity as much as possible.

4.2 Velocity and Temperature Contours for Flat Plate

After completing the simulation using ANSYS Fluent, these are the contours we have achieved. As we can see in the figures, figure 20 represents the temperature contour of the XY plane and figure 21 represents the temperature contour of the YZ plane of the flat plate.

The temperature distribution seems to be reasonable and conforms with the experimental results.
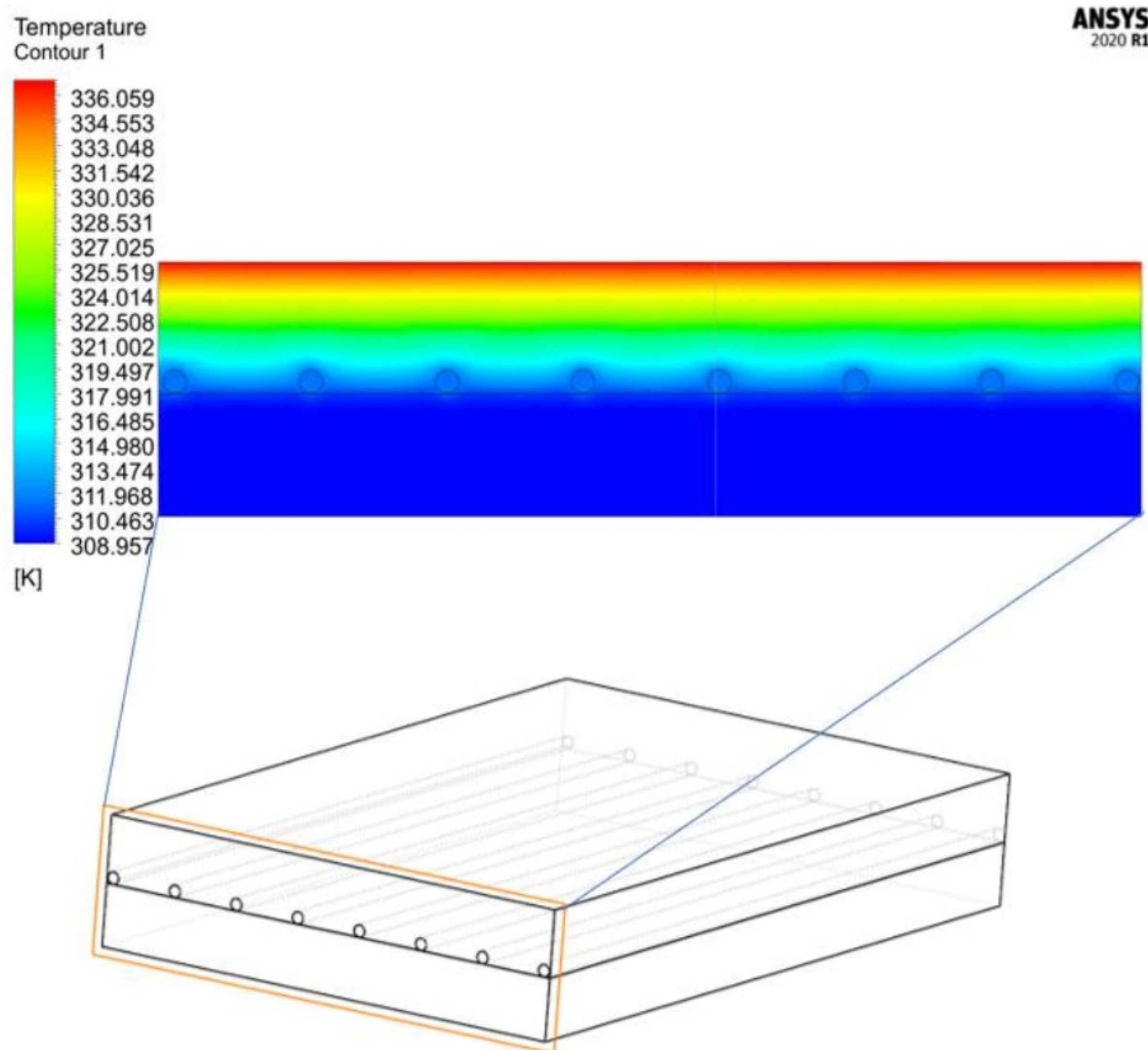
Figure 20: Temperature Contour of the XY plane of Flat Plate

From the figure 20 and 21, we can observe that the top surface of the computational domain has the highest temperature as it should be. Because the top surface is PV panel where the solar radiation falls. In the boundary condition we have provided the water inlet temperature from the experimental setup condition. As the temperature is maximum at the top surface the water heat exchangers seemed to gain some heat from above. We defined the absorber plate as Steel which is painted black. So, the absorber plate helps to attract heat and absorb it. Then it passed it to the water inside the copper tubes. This concept is the reason of us getting water outlet temperature higher as we provided all the necessary information before starting the simulation.

On the contrary air channel has the lowest temperature here as it has the maximum distance from the top surface. After observing the temperature contour plots, they seem reasonable and follow both the traditional concept and the experimental results.
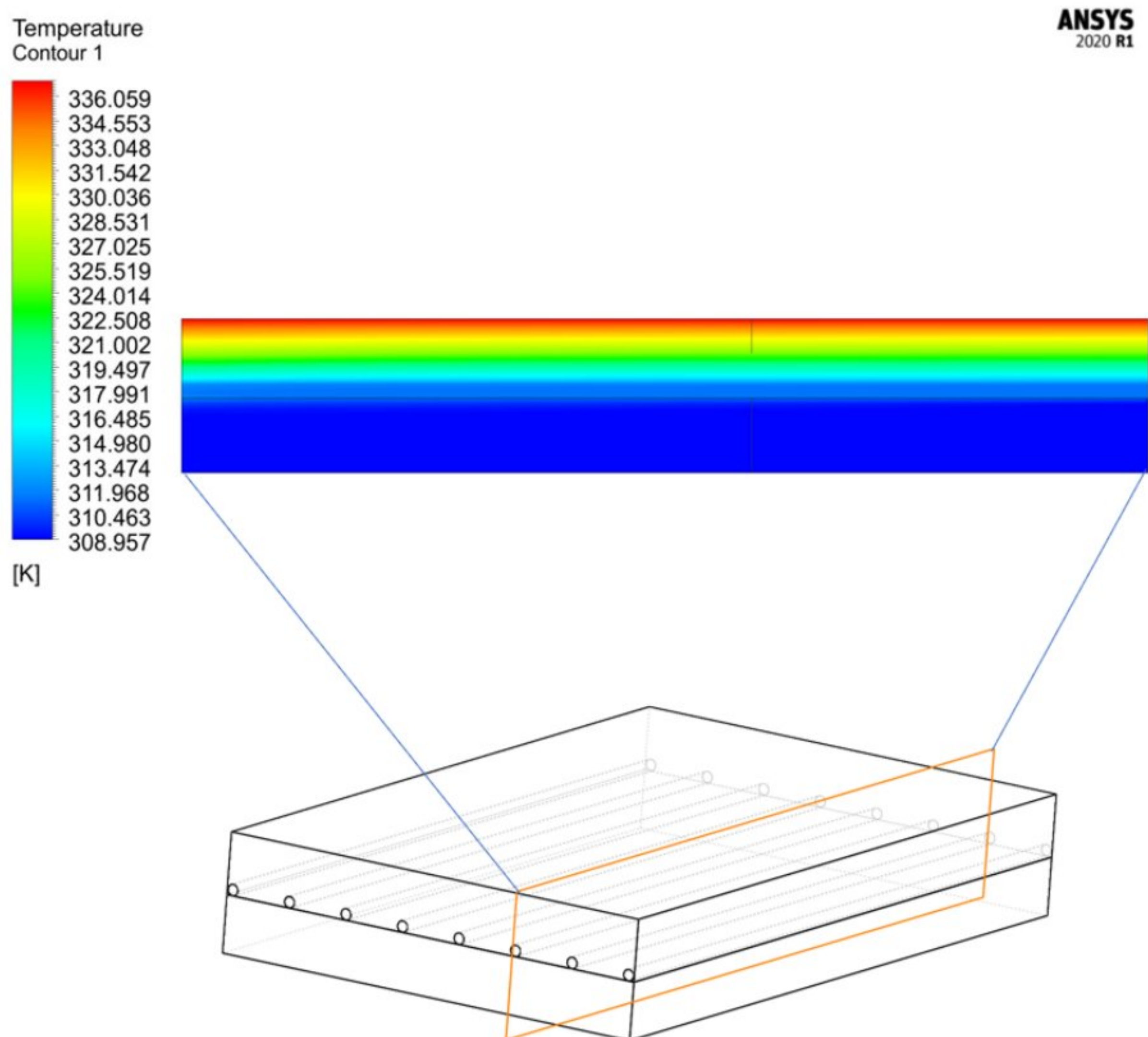
Figure 21: Temperature Contour of the YZ plane of Flat Plate
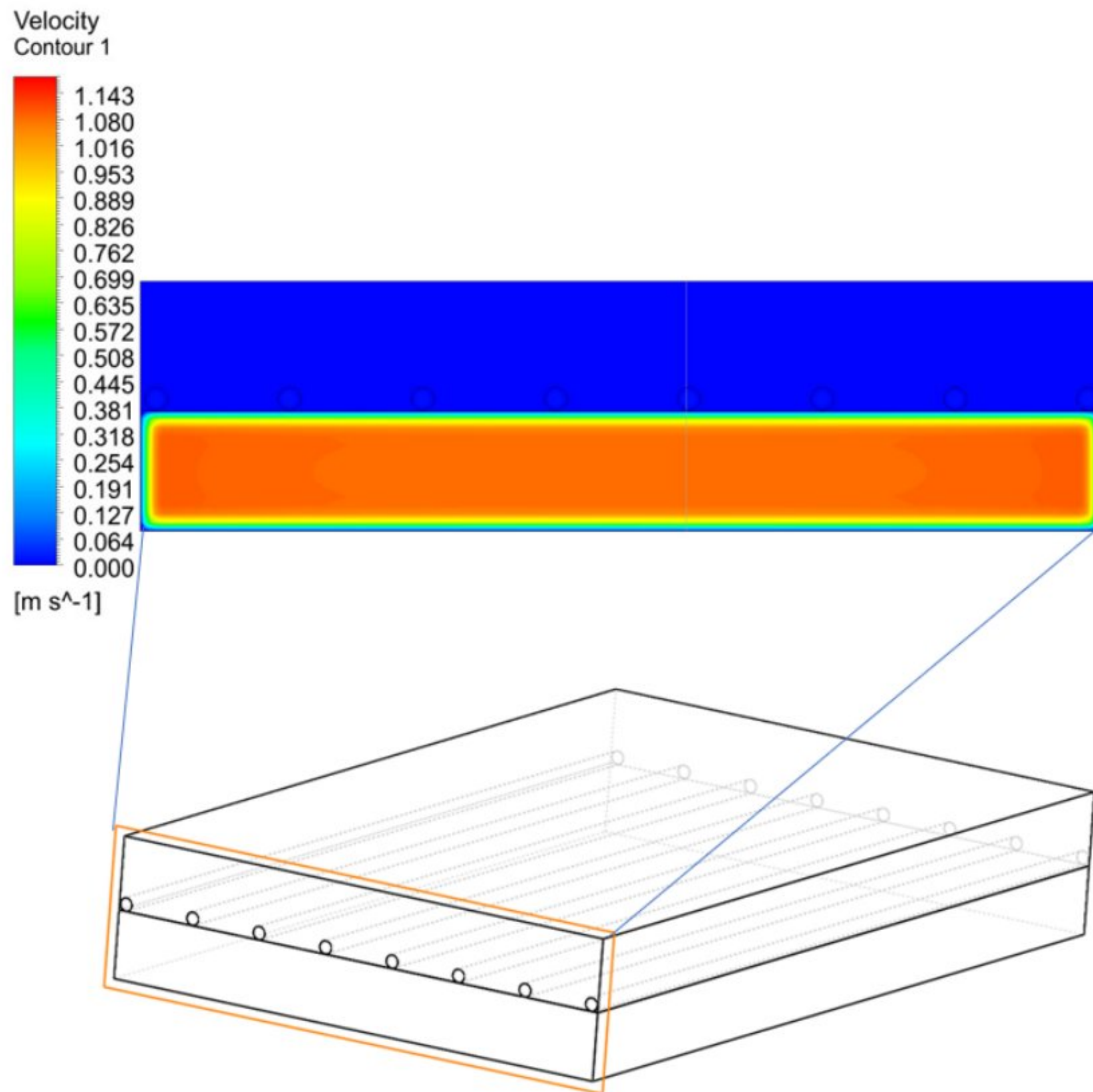
Figure 22: Velocity Contour of the XY plane of Flat Plate

Here Figure 22 indicates the velocity contour of the XY plane and figure 23 indicates the velocity contour of the YZ plane of flat plate. The upper part of the computational domain seems to have zero velocity which conforms with the experimental conditions as upper part is static air where velocity must be zero. In the lower part, which is air channel, the velocity seems to be increasing inwardly. This happened due to the no slip boundary condition at the four boundary walls of the air channel. The water tubes seem to have comparatively lower velocity as we specified in the boundary condition.

4.3 Comparison among the contours among all four geometries
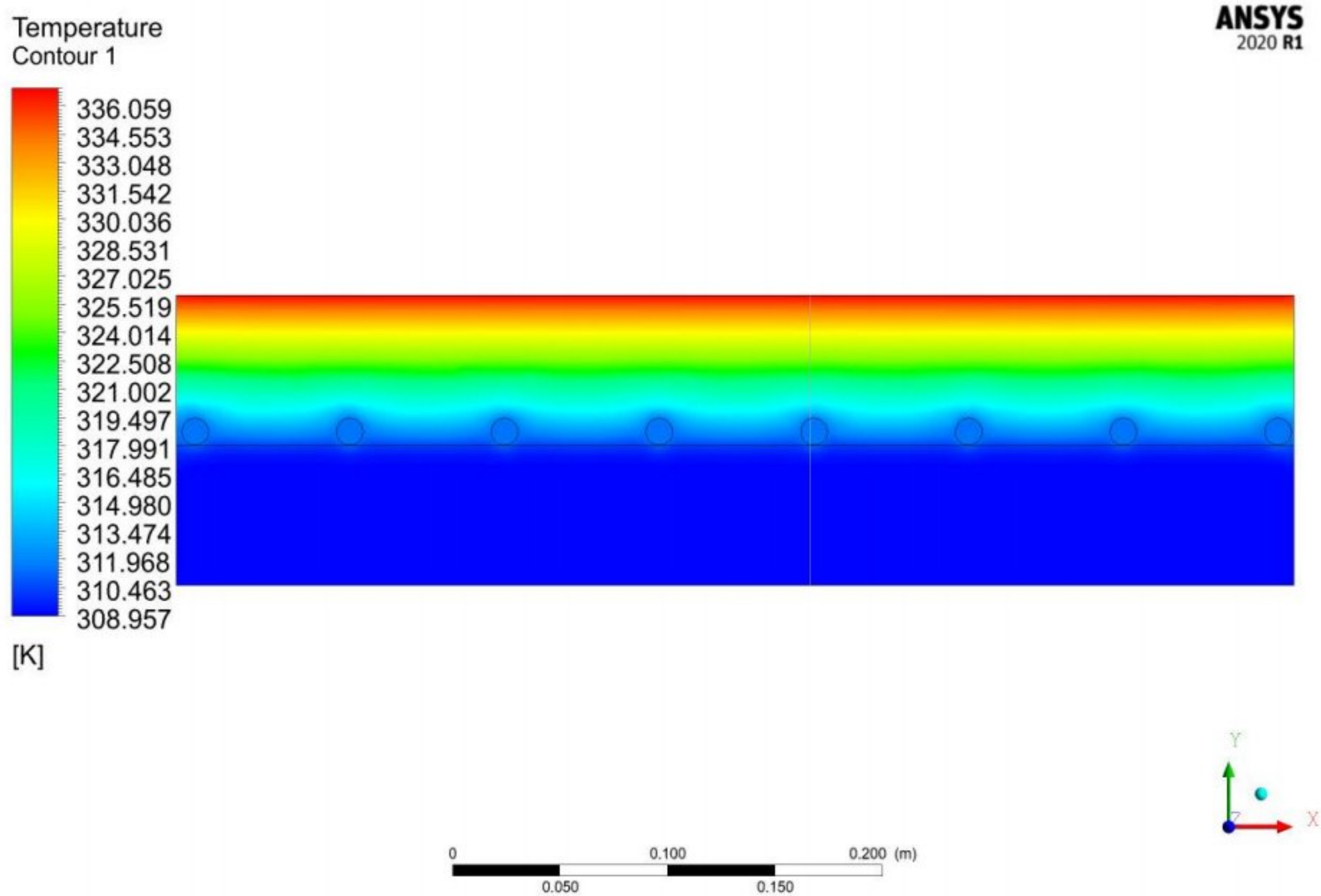
Figure 23: Temperature contour of the geometry with Flat plate [XY plane]
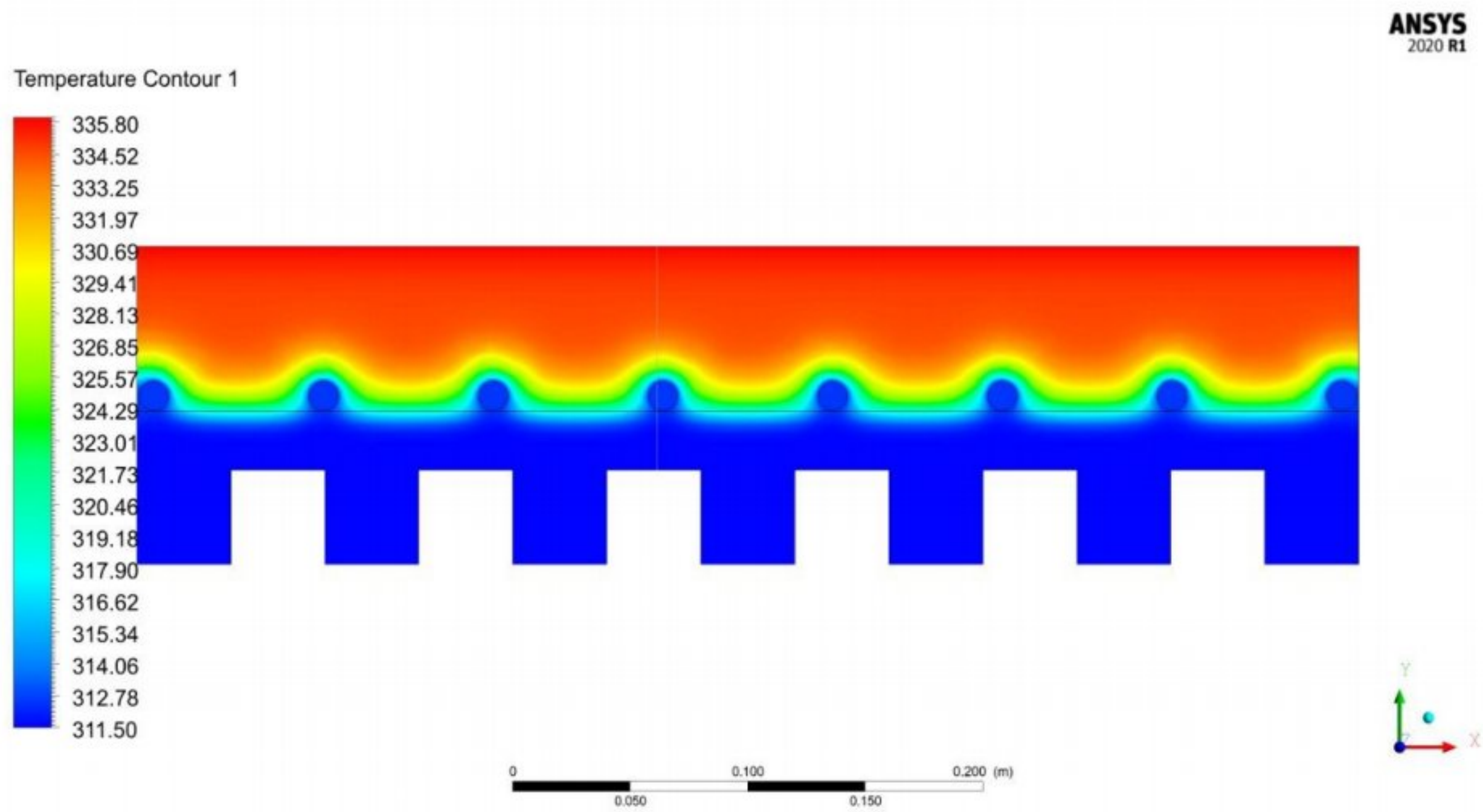
Figure 24: Temperature contour of the geometry with Rectangular Ribs [XY plane]
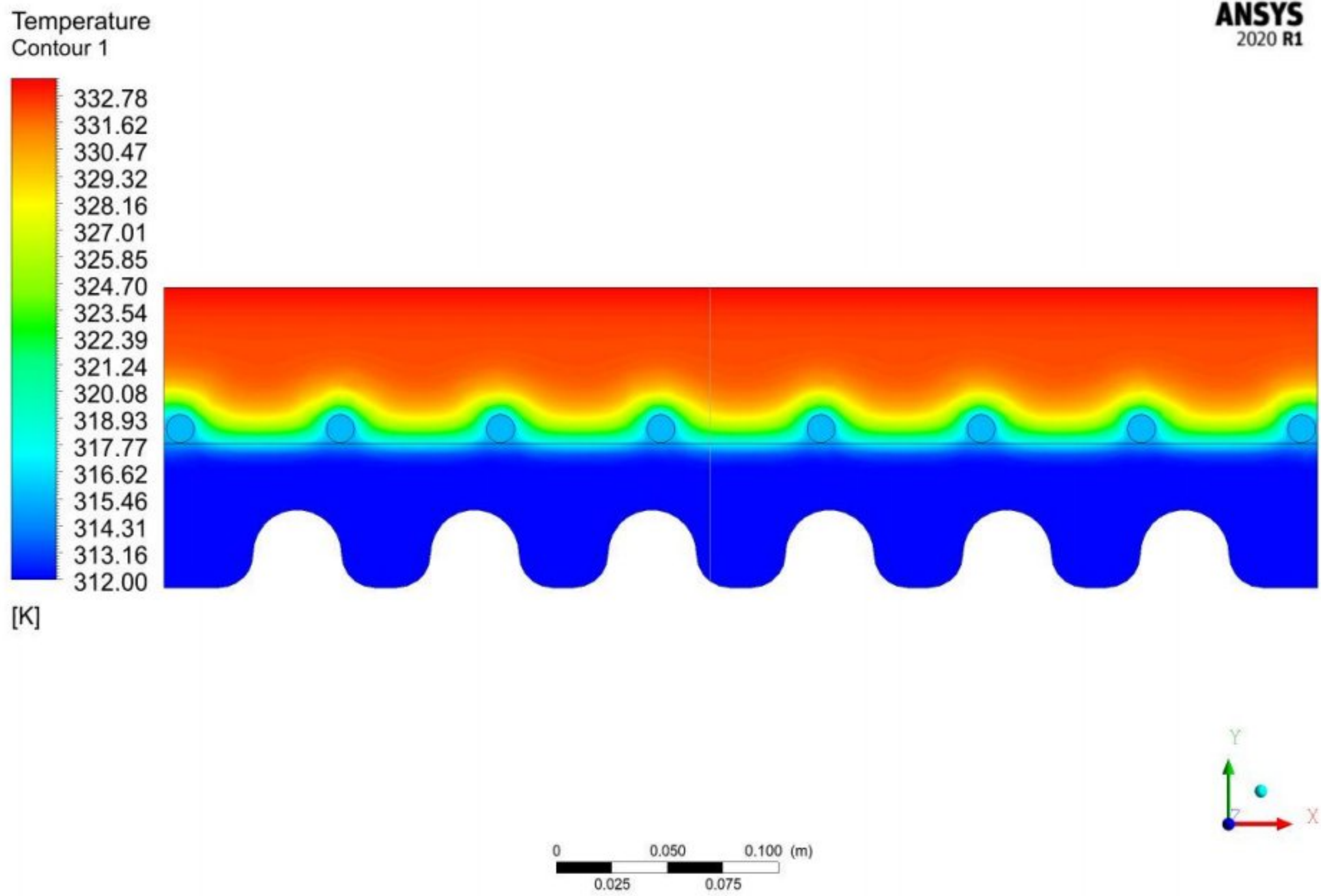
Figure 25: Temperature contour of the geometry with Semicircular Ribs [XY plane]
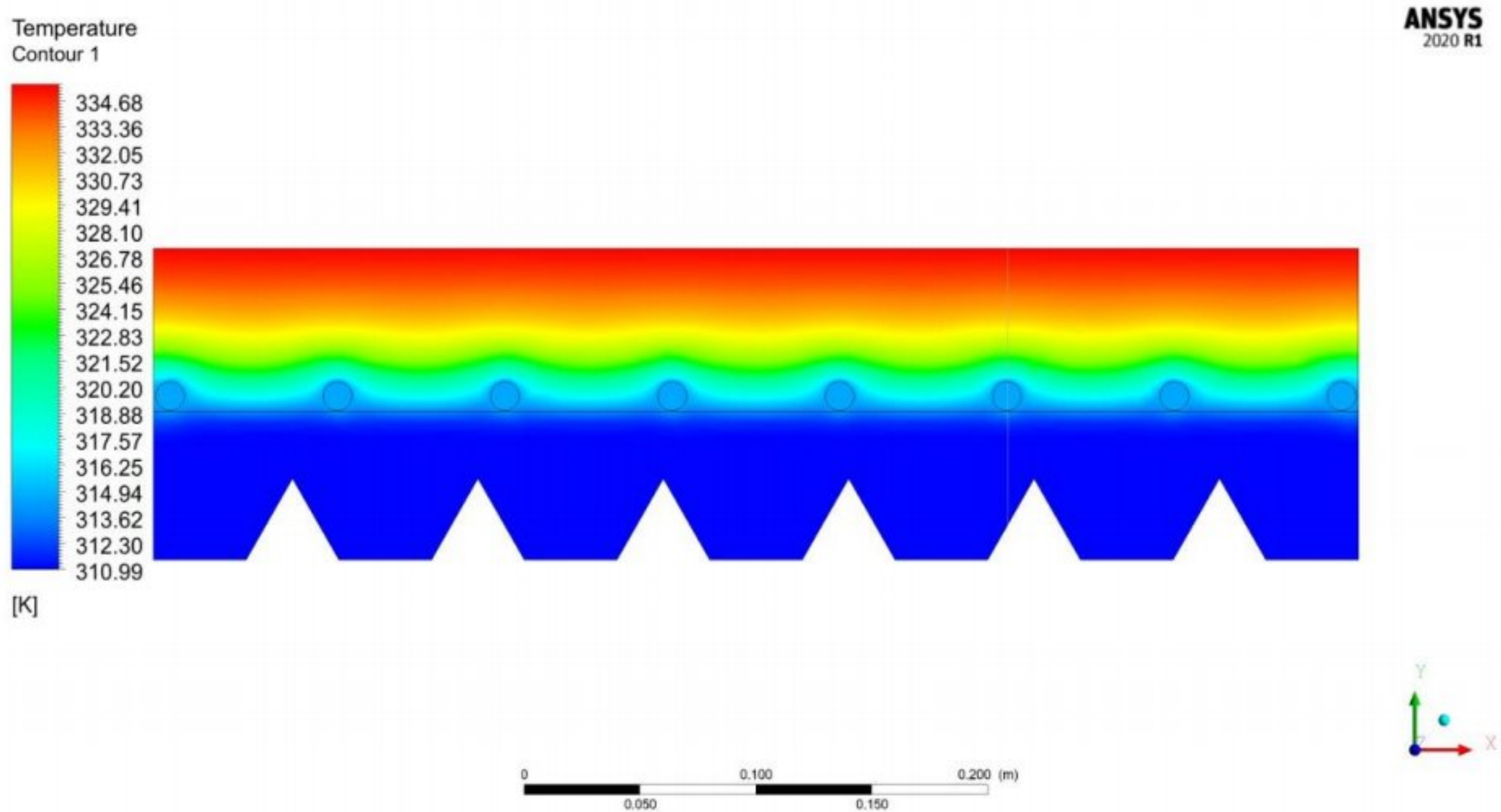
Figure 26: Temperature contour of the geometry with Triangular Ribs [XY plane]

If we compare the contours for all four geometries, we can see that for semicircular and triangular ribs, the water coolant has the tendency to achieve higher temperature as seen by observing the color spectrums at the outlet of the WHX. The temperatures of the water heat exchangers for semicircular and triangular ribs seem too higher than the others. It occurred because the area of the ribbed surfaces became larger, so they attracted more heat and as a result we achieved better results for geometries with semicircular and triangular ribs.

4.4 Deviation and percentage of relative error between the experimental and numerical results for all the geometries

Table 6: Flat Plate

Obs.	Time	Top Surface Temp. (K)	Air Inlet Temp. (K)	Water Inlet Temp. (K)	Water Outlet Temp. (K)		Relative Error %
					Paper	Numerical	
1	10:30 A.M	327	307.75	306	307.5	306.523	0.318
2	11:00 A.M	330	308	307.5	309	308	0.324
3	11:30 A.M	333	308.3	309	310	309.477	0.169
4	12:00 P.M	335	308.5	310	311	310.456	0.175
5	12:30 P.M	336.5	308.8	311	311.5	311.44	0.019
6	01:00 P.M	337	309	311.5	312	311.932	0.022

Table 7: Rectangular ribs

Obs.	Time	Top Surface Temp. (K)	Air Inlet Temp. (K)	Water Inlet Temp. (K)	Water Outlet Temp. (K)		Relative Error %
					Paper	Numerical	
1	10:30 A.M	326	308.6	308	309	308.448	0.179
2	11:00 A.M	329	309	309	310	309.498	0.162
3	11:30 A.M	333	309.5	310	311	310.567	0.139
4	12:00 P.M	335	310	311	312	311.682	0.102
5	12:30 P.M	336	311	312	312.5	312.424	0.024
6	01:00 P.M	336.5	311.5	312.5	313	312.707	0.094

Table 8: Semicircular ribs

Obs.	Time	Top Surface Temp. (K)	Air Inlet Temp. (K)	Water Inlet Temp. (K)	Water Outlet Temp. (K)		Relative Error %
					Paper	Numerical	
1	10:30 A.M	323	308.75	310	311	310.392	0.195
2	11:00 A.M	325	309	311	312	311.421	0.186
3	11:30 A.M	329	310	312	313.8	313.182	0.197
4	12:00 P.M	333	311	313.8	315	314.497	0.160
5	12:30 P.M	334	311.7	315	315.5	315.416	0.027
6	01:00 P.M	335.5	312	315.5	316	315.735	0.084

Table 9: Triangular ribs

Obs.	Time	Top Surface Temp. (K)	Air Inlet Temp. (K)	Water Inlet Temp. (K)	Water Outlet Temp. (K)		Relative Error %
					Paper	Numerical	
1	10:30 A.M	324.5	308.4	311	312	311.504	0.159
2	11:00 A.M	327	308.6	312	313	312.529	0.150
3	11:30 A.M	330.5	308.75	313	313.8	313.562	0.076
4	12:00 P.M	334	309	313.8	314	313.951	0.016
5	12:30 P.M	335.5	310.3	314	314.5	314.407	0.030
6	01:00 P.M	335.5	311	314.5	315	314.903	0.031

Relative error was calculated in these four tables. The results show that the maximum relative error that we have found is 0.324 % for Flat plate. The acceptable relative error is up to 5 %. But we achieved way less than the upper limit. So, all the calculated relative errors are in acceptable range. So, we can conclude that our numerical validation of the experimental setup is correct.

Chapter 05: CONCLUSION AND RECOMMENDATION

5.1 Conclusion and findings

Photovoltaic thermal collector, PVT systems are modified hybrid PV modules developed in order to compensate for the low electrical efficiency of the PV panel by successfully reducing the rising temperature of the solar cells caused by absorption of solar radiation and simultaneously generate a thermal output to enhance thermal efficiency. In this study a hybrid PV module with dual cooling system that simultaneously uses air and water as heat extraction fluids have been developed and numerically investigated for performance analysis.

From this research we can come to the following conclusions:

1. The outlet temperature of the water is maximum at 1:00 PM for all geometries when the top surface of the PV panel is at its highest temperature. This might be due to the fact that higher temperatures correspond to greater heat transfer rates and thus more thermal gain of cooing fluid. At this time solar heat flux is maximum resulting in lower electrical efficiency so greater water outlet temperature indicates better performance.

2. From the simulations, semicircular and triangular ribbed surfaces provided higher temperature gain compared to flat plate and rectangular ribbed surface which conformed with experimental results of previous works. Ribbed surfaces increase surface area and thus enhances heat transfer rate to the coolant achieving lower PV module temperature and greater thermal gain of the coolant.

3. Greater temperature gain of water outlet signifies more heat energy absorption indicating lower PV panel temperature and thus higher electrical efficiency and better performance of the PVT module. In addition, higher difference in water temperature effectively increases the thermal efficiency and is better for domestic and industrial utilization.

4. Water Outlet Temperature significantly decreases with increasing air velocity and decreasing water velocity. Thus, forced air circulation can effectively improve heat transfer and achieve better PVT performance. However, due to its lower density and heat capacity the enhancement in performance by increasing air velocity alone is limited.

5. The water flow velocity should be kept minimum to achieve greater thermal gain of water and better thermal and electrical efficiencies. The high heat capacity of water results in better heat gain at lower velocities and thus natural circulation of water is preferred. Furthermore, the thermal efficiency enhances with increasing temperature gain of the cooling fluid.

6. The simulation results validate experimental results for all geometries and conform to the results of previous studies. Comparison graphs showed similar trends for all geometries. The results from the numerical analysis had almost identical trends when compared to experimental data with slight errors that were minimum around noon and maximum in the morning.

5.2 Limitation and Sources of errors with recommendations for prevention

- Once it is established that the results of simulations are consistent with the analytical or mathematical model, it's very important to check the level of numerical errors. There could be various types of numerical errors in the ANSYS fluent simulation such as physical modeling and geometry modeling error, linearization error, spatial discretization, and temporal discretization errors etc. These are all basically acknowledged errors which means there are ways to identify and eliminate them. The linearization error is occurred when the solver is ended up with some non-linear algebraic equations and linearization must be done to achieve the solution. This type of error can be eliminated by iteration and updating the guessed values for different parameters like velocity, temperature, pressure etc. upon completion of each iteration. The iterations should be stopped Once the aggregate imbalances for mass, momentum and energy conservation fall below the tolerance level. According to the scaled residuals plot from figure 12, it can be observed that the continuity residual or the aggregate mass imbalance in case of each cell is normalized in the initial few iterations and the imbalance seems to be of order one, which is eventually reduced more than by six orders of magnitude, as the criteria was preset to be after six. The energy has reduced by six orders of magnitude, whereas other residuals like velocities in the x, y, and z directions have decreased to lesser orders than that. Since the imbalances dropped down to the

order six provides an acceptable range of linearization error, the absolute criteria were preset in such way earlier. The default was set to be at the order of three. However, it's not considered to be an acceptably low level of imbalances or residuals, resulting into significant linearization errors. Another way of preventing such errors is to observe the changes in drag coefficient when the imbalances are reduced by three orders of magnitude. On the other hand, for reducing the discretization error, it should be ensured that a 2nd order scheme is being used. The discretization error is introduced while converting the integral form into algebraic equations. For the second order methods, the error is decreased by a factor of 1/4th while reducing the spacing of the mesh by half.

- Another major source of error could be originated for not refining the mesh by using more control volumes and cells. When the mesh is coarse, it might result into larger discretization error. In the ANSYS meshing software, the mesh could be coarsened by reducing the number of divisions for the meshing. Under the mesh statistics, there are number of nodes. For example, for grid size 5 under the boundary conditions for flat plate according to the grid independency test, the number of nodes or chunks was 912730. Moreover, the cell centered values must be calculated for all the solution parameters by solving this large number of algebraic equations through ANSYS fluent. If the setup is initialized and calculation is run again for the new sets of coarser mesh, the solution seemed to be converged faster. Therefore, it can be concluded that the linearization error could be reduced more quickly in case of the coarsened meshes. It could be another cause of concern that whether the amount of solution accuracy that's being compromised for adopting coarser mesh will substantially change the desired output results. If the results are investigated before and after coarsening the mesh, it will be found that there will be no considerable change in the results for the temperature and velocity contours and plots. However, parameters for whom the interpolated solution is differentiated, such as wall shear stress; the results are changed causing a loss in solution accuracy.

- Generally, if laminar flow model is used in case of turbulent flow, the solution should not be converged. In this case, the coolant flow especially the air flow sometimes might be turbulent. However, all the coolants for all the cases are

assumed to be laminar and viscous laminar model is used. Moreover, the solution seemed to be converged probably due to some mistakes, such as usage of exorbitantly coarse mesh, excessive stabilization, and poor convergence tolerances.

▪ In order to avoid simulations complexity, the water flow was considered to be single pass for a particular time period even though the water was being recirculated multiple times for each iteration in case of the experimental setup. It has been assumed that the flow is being recirculated after every 30 minutes throughout our numerical calculations, whereas in reality it might not be the case. This problem could be eliminated by approximation of the time by using the coolant velocity and the distance traveled by the water coolant, instead of randomly specifying the recirculation time interval as 30 minutes.

▪ The simulations for all the cases were considered to be steady. In order to decrease the computational time, the time dependent nature of the model was ignored. This issue could be solved by enabling the transient nature despite the higher computational time and cost.

▪ In case of the experimental setup, a considerable portion of heat transfer takes place through incoming solar radiation. However, in this study the heat transfer through solar radiation was not modelled for numerical analysis. This resulted in lower temperature gain of the water for the numerical results compared to that of the experimental results. This issue could be solved by taking the effects of solar radiation into consideration during the calculation of the heat flux limit at the PV panel top surface or collector region. [40]

5.3 Future Prospects and further scopes of improvements

- For the improvement of the performance of a PVT system, more attention has been paid to improve the thermal efficiency compared to the electrical efficiency. In order to improve the thermal performance, water cooled, air cooled, combination of water and air cooled, PCM based and hear pipes incorporated thermal PV systems are studied. The overall efficiency of a thermal PV system is enhanced if the water and nanoparticles are employed as base fluid. These various types of thermal PV systems must be studied further to compare their ability to enhance the thermal efficiency which in term decreases the PV module temperatures. Since the thermal analysis of PVT module requires more technical and financial support, further researches should be done to decrease the financial expense, increase the effectiveness and improve the technical design.[45]

- It has already been established that the efficiency of a solar photovoltaic system is decreased by 0.3 % for 1°C increase in the temperature of the PV module. As we know the solution to this kind of problem has been the thermal PVT hybrid systems for extracting the extra heat resulting into reduced temperature and improved performance. However, a new kind of heat exchanger can be used for typical solar PV and thermal PVT hybrid modules which is capable of effectively transferring heat to the circulating air. This results into a considerable improvement of open circuit voltage and the overall output power. Furthermore, researches should be conducted to design a more effective heat exchanger for the thermal PVT hybrid system which will result into more improved electrical performance. [46]

- Some research might be carried out by considering the relative roughness for the riser tubes or water heat exchangers, in the future. The pressure drop of the system can be calculated depending on the relative roughness of the pipes. Since the pressure drop has direct correlation with the range of coolant flow rate, [47] the relative roughness could be manipulated. In future, optimum performance for the hybrid thermal photovoltaic panel might be determined by studying the effects of the relative roughness.

- Here, only the effects of water cooling have been considered since for each case the desired output is the water outlet temperature. The more the temperature at the water outlet, the more the thermal and electrical efficiency. The enhancement in electrical efficiency due to air cooling could also be simulated and analyzed.

- The thermal efficiency of heat extraction could be improved further by employing different liquid working fluids such as Glycerin-water mixtures etc. It has been found that addition of glycerin to water leads to significant increase in the overall efficiency [38]. Further analysis could be done to find the appropriate liquid and the suitable ratio to be mixed with water for obtaining maximum efficiency through heat extraction

- The heat transfer by solar radiation should be modelled in future works to capture the real temperature gain value closer to that of the experimental data.

- It has been concluded from the earlier discussion that the more the air velocity, the more the heat transfer. Therefore, forced convection systems such as fans could be employed for the air coolant and the effects should be analyzed to extract more heat through the coolant compared to natural convection.

REFERENCES

[1]   "Solar Panel Construction — Clean Energy Reviews."
        https://www.cleanenergyreviews.info/blog/solar-panel-components-
        construction (accessed May 08, 2022).

[2]   "Working principle and Development of Solar Cell."
        https://www.apogeeweb.net/article/27.html (accessed May 08, 2022).

[3]   R. Gangadevi, S. Agarwal, and S. Roy, "A Novel Hybrid Solar System Using
        Nanofluid," *Int. J. Eng. Res. Technol.*, vol. 6, no. 6, pp. 747–752, 2013.

[4]   A. Makki, S. Omer, and H. Sabir, "Advancements in hybrid photovoltaic
        systems for enhanced solar cells performance," *Renew. Sustain. energy Rev.*,
        vol. 41, pp. 658–684, 2015.

[5]   Y. Kemmoku *et al.*, "Modelling of module temperature of a concentrator PV
        system," in *Proc. 19th European photovoltaic solar energy conference*, 2004,
        pp. 2568–2571.

[6]   T. T. Chow, "A review on photovoltaic/thermal hybrid solar technology," *Appl.
        Energy*, vol. 87, no. 2, pp. 365–379, 2010.

[7]   N. Aste, F. Leonforte, and C. Del Pero, "Simulation and model validation of
        uncovered PVT solar system," in *2013 International Conference on Clean
        Electrical Power (ICCEP)*, 2013, pp. 789–795.

[8]   N. Aste, G. Chiesa, and F. Verri, "Design, development and performance
        monitoring of a photovoltaic-thermal (PVT) air collector," *Renew. energy*, vol.
        33, no. 5, pp. 914–927, 2008.

[9]   N. Aste, C. Del Pero, and F. Leonforte, "Water flat plate PV–thermal
        collectors: a review," *Sol. Energy*, vol. 102, pp. 98–115, 2014.

[10]   J. J. Michael, S. Iniyan, and R. Goic, "Flat plate solar photovoltaic–thermal
        (PV/T) systems: a reference guide," *Renew. Sustain. energy Rev.*, vol. 51, pp.
        62–88, 2015.

[11]   P. G. Charalambous, G. G. Maidment, S. A. Kalogirou, and K. Yiakoumetti,
        "Photovoltaic thermal (PV/T) collectors: A review," *Appl. Therm. Eng.*, vol.
        27, no. 2–3, pp. 275–286, 2007.

[12]   M. Herrando, C. N. Markides, and K. Hellgardt, "A UK-based assessment of
        hybrid PV and solar-thermal systems for domestic heating and power: system
        performance," *Appl. Energy*, vol. 122, pp. 288–309, 2014.

[13]   "Solimpeks hybrid solar PV-thermal modules in Australia - Solar Choice."
        https://www.solarchoice.net.au/blog/solimpeks-hybrid-pv-thermal-solar-
        panels-in-australia/ (accessed May 08, 2022).

[14]   G. L. Jin *et al.*, "Evaluation of single-pass photovoltaic-thermal air collector
        with rectangle tunnel absorber," *Am. J. Appl. Sci.*, vol. 7, no. 2, pp. 277–282,
        2010, doi: 10.3844/ajassp.2010.277.282.

[15]   M. E. A. Alfegi, K. Sopian, M. Y. H. Othman, and B. Bin Yatim,
        "Experimental investigation of single pass, double duct photovoltaic thermal
        (PV/T) air collector with CPC and fins," *Am. J. Appl. Sci.*, vol. 5, no. 7, pp.
        866–871, 2008, doi: 10.3844/ajassp.2008.866.871.

[16]   P. Rawat, M. Debbarma, S. Mehrotra, K. Sudhakar, E. Centre, and M. Pradesh,
        "Design , Development and Experimental Investigation of Solar Photovoltaic /
        Thermal (Pv / T) Water," *Ijset.Net*, vol. 3, no. 3, pp. 1173–1183, 2014,
        [Online]. Available: www.ijset.net.

[17]   J. I. Bilbao and A. B. Sproul, "Experimental Results of a Pvt-Water Module
        Design for Developing Countries," *proceeding 50th Annu. Conf. Aust. Sol.
        Energy Soc.*, no. December, pp. 1–11, 2012.

[18] P. Dupeyrat, C. Ménézo, H. Wirth, and M. Rommel, "Improvement of PV module optical properties for PV-thermal hybrid collector application," *Sol. Energy Mater. Sol. Cells*, vol. 95, no. 8, pp. 2028–2036, 2011, doi: 10.1016/j.solmat.2011.04.036.

[19] K. Touafek, M. Haddadi, and A. Malek, "Experimental study on a new hybrid photovoltaic thermal collector," *Appl. Sol. Energy (English Transl. Geliotekhnika)*, vol. 45, no. 3, pp. 181–186, 2009, doi: 10.3103/S0003701X09030104.

[20] T. T. Chow, G. Pei, K. F. Fong, Z. Lin, A. L. S. Chan, and J. Ji, "Energy and exergy analysis of photovoltaic – thermal collector with and without glass cover," *Appl. Energy*, vol. 86, no. 3, pp. 310–316, 2009, doi: 10.1016/j.apenergy.2008.04.016.

[21] T. Fujisawa and T. Tani, "Annual exergy evaluation on photovoltaic-thermal hybrid collector," *Sol. Energy Mater. Sol. Cells*, vol. 47, no. 1–4, pp. 135–148, 1997, doi: 10.1016/S0927-0248(97)00034-2.

[22] J. K. Tonui and Y. Tripanagnostopoulos, "Improved PV/T solar collectors with heat extraction by forced or natural air circulation," *Renew. Energy*, vol. 32, no. 4, pp. 623–637, 2007, doi: 10.1016/j.renene.2006.03.006.

[23] R. Liang, J. Zhang, L. Ma, and Y. Li, "Performance evaluation of new type hybrid photovoltaic/thermal solar collector by experimental study," *Appl. Therm. Eng.*, vol. 75, pp. 487–492, 2015, doi: 10.1016/j.applthermaleng.2014.09.075.

[24] M. A. R. Akhanda, "Study of a hybrid photovoltaic thermal (PVT) solar systems using different ribbed surfaces opposite to absorber plate Study of a hybrid photovoltaic thermal (PVT) solar systems using different ribbed surfaces opposite to absorber plate," vol. 9, no. January 2011, pp. 1–14, 2014.

[25] M. Al-Damook *et al.*, "CFD analysis of a one-pass photovoltaic/thermal air system with and without offset strip fins," *MATEC Web Conf.*, vol. 240, 2018, doi: 10.1051/matecconf/201824003002.

[26] N. Aste, C. Del Pero, and F. Leonforte, "Water PVT Collectors Performance Comparison," *Energy Procedia*, vol. 105, pp. 961–966, 2017, doi: 10.1016/j.egypro.2017.03.426.

[27] M. Y. Othman, B. Yatim, K. Sopian, and M. N. Abu Bakar, "Performance studies on a finned double-pass photovoltaic-thermal (PV/T) solar collector," *Desalination*, vol. 209, no. 1-3 SPEC. ISS., pp. 43–49, 2007, doi: 10.1016/j.desal.2007.04.007.

[28] S. Hassani, R. A. Taylor, S. Mekhilef, and R. Saidur, "A cascade nanofluid-based PV/T system with optimized optical and thermal properties," *Energy*, vol. 112, pp. 963–975, 2016, doi: 10.1016/j.energy.2016.06.142.

[29] Z. Han, K. Liu, G. Li, X. Zhao, and S. Shittu, "Electrical and thermal performance comparison between PVT-ST and PV-ST systems," *Energy*, vol. 237, p. 121589, 2021, doi: 10.1016/j.energy.2021.121589.

[30] J. Guo and L. Zheng, "Numerically study on a new hybrid photovoltaic thermal (PVT) collectors with natural circulation," *Appl. Sol. Energy (English Transl. Geliotekhnika)*, vol. 53, no. 4, pp. 316–321, 2017, doi: 10.3103/S0003701X17040077.

[31] H. A. Zondag, D. W. D. E. Vries, W. G. J. V. A. N. Helden, R. J. C. V. A. N. Zolingen, and A. A. V. A. N. Steenhoven, "THE THERMAL AND ELECTRICAL YIELD OF A PV-THERMAL COLLECTOR," vol. 72, no. 2, pp. 113–128, 2002.

[32] G. Fraisse and K. Johannes, "Energy performance of water hybrid PV / T collectors applied to combisystems of Direct Solar Floor type," vol. 81, pp. 1426–1438, 2007, doi: 10.1016/j.solener.2006.11.017.

[33] M. Bakker, H. A. Zondag, M. J. Elswijk, K. J. Strootman, and M. J. M. Jong, "Performance and costs of a roof-sized PV/thermal array combined with a ground coupled heat pump," *Sol. Energy*, vol. 78, no. 2, pp. 331–339, 2005, doi: 10.1016/j.solener.2004.09.019.

[34] M. Carmona, A. Palacio Bastos, and J. D. García, "Experimental evaluation of a hybrid photovoltaic and thermal solar energy collector with integrated phase change material (PVT-PCM) in comparison with a traditional photovoltaic (PV) module," *Renew. Energy*, vol. 172, pp. 680–696, 2021, doi: 10.1016/j.renene.2021.03.022.

[35] R. M. da Silva and J. L. M. Fernandes, "Hybrid photovoltaic/thermal (PV/T) solar systems simulation with Simulink/Matlab," *Sol. Energy*, vol. 84, no. 12, pp. 1985–1996, 2010, doi: 10.1016/j.solener.2010.10.004.

[36] C.-Y. Huang and C.-J. Huang, "A study of photovoltaic thermal (PV/T) hybrid system with computer modeling," *Int. J. Smart Grid Clean Energy*, vol. 3, no. 1, pp. 75–79, 2014, doi: 10.12720/sgce.3.1.75-79.

[37] I. Karaaslan and T. Menlik, "Numerical study of a photovoltaic thermal (PV/T) system using mono and hybrid nanofluid," *Sol. Energy*, vol. 224, no. March, pp. 1260–1270, 2021, doi: 10.1016/j.solener.2021.06.072.

[38] M. Mourshed, S. Kumar Ghosh, T. Islam, and N. Nath Mustafi, "Experimental investigation and CFD analysis of a solar hybrid PV/T system for the sustainable development of the rural northern part of Bangladesh," *Int. J. Sustain. Energy*, vol. 38, no. 6, pp. 583–602, 2019, doi: 10.1080/14786451.2018.1548465.

[39] H. Bahaidarah, A. Subhan, P. Gandhidasan, and S. Rehman, "Performance evaluation of a PV (photovoltaic) module by back surface water cooling for hot climatic conditions," *Energy*, vol. 59, pp. 445–453, 2013, doi: 10.1016/j.energy.2013.07.050.

[40] A. Khelifa, K. Touafek, H. Ben Moussa, I. Tabet, H. B. C. El Hocine, and H. Haloui, "Analysis of a Hybrid Solar Collector Photovoltaic Thermal (PVT)," *Energy Procedia*, vol. 74, pp. 835–843, 2015, doi: 10.1016/j.egypro.2015.07.819.

[41] D. S. Strebkov and N. S. Filippchenkova, "Results of CFD-simulation of a solar photovoltaic-thermal module," *IOP Conf. Ser. Earth Environ. Sci.*, vol. 659, no. 1, 2021, doi: 10.1088/1755-1315/659/1/012113.

[42] I. R. Caluianu and F. Bălătreţu, "Thermal modelling of a photovoltaic module under variable free convection conditions," *Appl. Therm. Eng.*, vol. 33–34, no. 1, pp. 86–91, 2012, doi: 10.1016/j.applthermaleng.2011.09.016.

[43] K. Narrein and H. A. Mohammed, "Influence of nanofluids and rotation on helically coiled tube heat exchanger performance," *Thermochim. Acta*, vol. 564, pp. 13–23, 2013, doi: 10.1016/j.tca.2013.04.004.

[44] K. Narrein and H. A. Mohammed, "Influence of nanofluids and rotation on helically coiled tube heat exchanger performance," *Thermochim. Acta*, vol. 564, pp. 13–23, 2013, doi: 10.1016/j.tca.2013.04.004.

[45] A. H. A. Al-Waeli, K. Sopian, H. A. Kazem, and M. T. Chaichan, "Photovoltaic/Thermal (PV/T) systems: Status and future prospects," *Renew. Sustain. Energy Rev.*, vol. 77, no. March, pp. 109–130, 2017, doi: 10.1016/j.rser.2017.03.126.

[46] R. Hossain *et al.*, "New Design of Solar Photovoltaic and Thermal Hybrid System for Performance Improvement of Solar Photovoltaic," *Int. J. Photoenergy*, vol. 2020, no. 1, 2020, doi: 10.1155/2020/8825489.

[47] J. Allan, "The development and characterisation of enhanced hybrid solar photovoltaic thermal systems," *Sol. energy*, no. May, 2015.